

NISTIR 5709

# Electronics and Electrical Engineering Laboratory

# Technical Progress Bulletin

J. M. Rohrbaugh  
Compiler

Covering Laboratory Programs,  
April to June 1995  
with 1995 EEEL Events Calendar

# 95-2

U.S. DEPARTMENT OF COMMERCE  
Technology Administration  
National Institute of Standards  
and Technology



QC  
100  
.U56  
NO.5709  
1995



NISTIR 5709

# Electronics and Electrical Engineering Laboratory

J. M. Rohrbaugh  
Compiler

Electronics and Electrical  
Engineering Laboratory  
Semiconductor Electronics Division  
Gaithersburg, MD 20899

# Technical Progress Bulletin

September 1995

Covering Laboratory Programs,  
April to June 1995  
with 1995 EEEL Events Calendar

# 95-2



U.S. DEPARTMENT OF COMMERCE  
Ronald H. Brown, Secretary  
TECHNOLOGY ADMINISTRATION  
Mary L. Good, Under Secretary for  
Technology  
NATIONAL INSTITUTE OF STANDARDS  
AND TECHNOLOGY  
Arati Prabhakar, Director

**ELECTRONICS AND ELECTRICAL ENGINEERING LABORATORY  
TECHNICAL PROGRESS BULLETIN, SEPTEMBER 1995 ISSUE**

**INTRODUCTION**

This is the fifty-first issue of a quarterly publication providing information on the technical work of the National Institute of Standards and Technology Electronics and Electrical Engineering Laboratory (EEEL). This issue of the EEEL Technical Progress Bulletin covers the second quarter of calendar year 1995.

Organization of Bulletin: This issue contains abstracts for all relevant papers released for publication by NIST in the quarter and citations and abstracts for such papers published in the quarter. Entries are arranged by technical topic as identified in the Table of Contents and alphabetically by first author under each subheading within each topic. Unpublished papers appear under the subheading "Released for Publication." This does not imply acceptance by any outside organization. Papers published in the quarter appear under the subheading "Recently Published." Following each abstract is the name and telephone number of the individual to contact for more information on the topic (usually the first author). This issue also includes a calendar of Laboratory conferences and workshops planned for calendar year 1995 and a list of sponsors of the work.

Electronics and Electrical Engineering Laboratory: EEEL programs provide national reference standards, measurement methods, supporting theory and data, and traceability to national standards. The metrological products of these programs aid economic growth by promoting equity and efficiency in the marketplace, by removing metrological barriers to improved productivity and innovation, by increasing U.S. competitiveness in international markets through facilitation of compliance with international agreements, and by providing technical bases for the development of voluntary standards for domestic and international trade. These metrological products also aid in the development of rational regulatory policy and promote efficient functioning of technical programs of the Government.

The work of the Laboratory is conducted by five technical research Divisions: the Semiconductor Electronics and the Electricity Divisions in Gaithersburg, Md., and the Electromagnetic Fields and the Electromagnetic Technology Divisions, and the newly formed Optoelectronics Division in Boulder, Colo. The Office of Law Enforcement Standards conducts research and provides technical services to the U.S. Department of Justice and State and local governments, and other agencies in support of law enforcement activities. In addition, the Office of Microelectronics Programs (OMP) coordinates the growing number of semiconductor-related research activities at NIST. Reports of work funded through the OMP are included under the heading "Semiconductor Microelectronics."

Key contacts in the Laboratory are listed at the end of this publication; readers are encouraged to contact any of these individuals for further information. To request a subscription or for more information on the Bulletin, write to EEEL Technical Progress Bulletin, National Institute of Standards and Technology, Metrology Building, Room B-358, Gaithersburg, MD 20899 or call (301) 975-2220.

Laboratory Sponsors: The Laboratory Programs are sponsored by the National Institute of Standards and Technology and a number of other organizations, in both the Federal and private sectors; these are identified on page 30.

Note on Publication Lists: Publication lists covering the work of each division are guides to earlier as well as recent work. These lists are revised and reissued on an approximately annual basis and are available from the originating division. The current set is identified in the Additional Information section, page 29.

---

Certain commercial equipment, instruments, or materials are identified in this paper in order to specify adequately the experimental procedures. Such identification does not imply recommendation or endorsement by the National Institute of Standards and Technology, nor does it imply that the materials or equipment identified are necessarily the best available for the purpose.

## TABLE OF CONTENTS

|  |    |
|--|----|
| INTRODUCTION .....   | ii |
| FUNDAMENTAL ELECTRICAL MEASUREMENTS .....                              | 3  |
| SEMICONDUCTOR MICROELECTRONICS .....                                   | 4  |
| Silicon Materials [includes SIMOX and SOI] .....                       | 4  |
| Compound Materials .....   | 5  |
| Analysis and Characterization Techniques .....                         | 5  |
| Device Physics and Modeling .....                                      | 5  |
| Insulators and Interfaces .....  | 6  |
| Dimensional Metrology .....  | 7  |
| Microfabrication Technology [includes MBE, micromachining, MEMs] ..... | 7  |
| Plasma Processing .....  | 7  |
| Photodetectors .....   | 9  |
| Reliability [includes electromigration] .....                          | 9  |
| SIGNAL ACQUISITION, PROCESSING, AND TRANSMISSION .....                 | 11 |
| DC and Low-Frequency Metrology .....                                   | 11 |
| Waveform Metrology .....   | 12 |
| Cryoelectronic Metrology .....   | 13 |
| Antenna Metrology [includes radar cross section measurements] .....    | 15 |
| Microwave and Millimeter-Wave Metrology .....                          | 16 |
| Electromagnetic Properties .....                                       | 17 |
| Laser Metrology .....  | 19 |
| Optical Fiber Metrology .....  | 19 |
| Optical Fiber/Waveguide Sensors .....                                  | 20 |
| Integrated Optics [includes waveguide structures] .....                | 21 |
| Complex System Testing .....   | 21 |
| Other Signal Topics .....  | 21 |
| ELECTRICAL SYSTEMS .....   | 22 |
| Power Systems Metrology .....  | 22 |
| Magnetic Materials and Measurements .....                              | 25 |
| Superconductors .....  | 26 |
| ELECTROMAGNETIC INTERFERENCE .....                                     | 27 |
| Conducted EMI .....  | 27 |
| Radiated EMI .....   | 27 |
| PRODUCT DATA SYSTEMS .....   | 28 |
| VIDEO TECHNOLOGY .....   | 28 |
| ADDITIONAL INFORMATION .....   | 29 |
| List of Publications .....   | 29 |
| 1995 Calendar of Events .....  | 30 |
| EEEL Sponsors .....  | 30 |

## TO LEARN MORE ABOUT THE LABORATORY....

Two general documents are available that may be of interest. These are *Measurements for Competitiveness in Electronics* and *EEEL 1994 Technical Accomplishments, Supporting Technology for U.S. Competitiveness in Electronics*. The first identifies measurement needs for a number of technical areas and the general importance of measurements to competitiveness issues. The findings of each chapter dealing with an individual industry have been reviewed by members of that industry. The second presents selected technical accomplishments of the Laboratory for the period October 1, 1993 through September 30, 1994. A brief indication of the nature of the technical achievement and the rationale for its undertaking are given for each example. A longer description of both documents follows:

### **Measurements for Competitiveness in Electronics, NISTIR 4583 (April 1993).**

*Measurements for Competitiveness in Electronics* identifies for selected technical areas the measurement needs that are most critical to U.S. competitiveness, that would have the highest economic impact if met, and that are the most difficult for the broad range of individual companies to address. The document has two primary purposes: (1) to show the close relationship between U.S. measurement infrastructure and U.S. competitiveness and show why improved measurement capability offers such high economic leverage, and (2) to provide a statement of the principal measurement needs affecting U.S. competitiveness for given technical areas, as the basis for a possible plan to meet those needs, should a decision be made to pursue this course.

The first three chapters, introductory in nature, cover the areas of: the role of measurements in competitiveness, NIST's role in measurements, and an overview of U.S. electronics and electrical-equipment industries. The remaining nine chapters address individual fields of electronic technology: semiconductors, magnetics, superconductors, microwaves, lasers, optical-fiber communications, optical-fiber sensors, video, and electromagnetic compatibility. Each of these nine chapters contains four basic types of information: technology review, world markets and U.S. competitiveness, goals of U.S. industry for competitiveness, and measurement needs. Three appendices provide definitions of the U.S. electronics and electrical-equipment industries.

This document is a successor to NISTIR 90-4260, *Emerging Technologies in Electronics ... and their measurement needs* [Second Edition].

[Contact: Ronald M. Powell, (301) 975-2220]

### **EEEL 1994 Technical Accomplishments, Supporting Technology for U.S. Competitiveness in Electronics, NISTIR 5551 (December 1994).**

The Electronics and Electrical Engineering Laboratory, working in concert with other NIST Laboratories, is providing measurement and other generic technology critical to the competitiveness of the U.S. electronics industry and the U.S. electricity-equipment industry. This report summarizes selected technical accomplishments and describes activities conducted by the Laboratory in FY 1994 in the field of semiconductors, magnetics, superconductors, low-frequency microwaves, lasers, optical fiber communications and sensors, video, power, electromagnetic compatibility, electronic data exchange, and national electrical standards. Also included is a profile of EEEL's organization, its customers, and the Laboratory's long-term goals.

EEEL is comprised of five technical divisions, Electricity and Semiconductor Electronics in Gaithersburg, Maryland, and Electromagnetic Fields, Electromagnetic Technology, and Optoelectronics in Boulder, Colorado. Through two offices, the Laboratory manages NIST-wide programs in microelectronics and law enforcement.

[Contact: JoAnne Surette, (301) 975-5267]

**FUNDAMENTAL ELECTRICAL MEASUREMENTS**

Released for Publication

**Kautz, R.L., Shapiro Steps in Large-Area Metallic-Barrier Josephson Junctions.**

The current amplitudes of Shapiro steps are investigated in large-area metallic-barrier Josephson junctions, both with and without a ground plane, with the goal of optimizing junction parameters for programmable voltage standards. Using the resistively shunted junction model without capacitance, we calculate maximum step amplitudes as a function of reduced frequency and junction dimension for both one- and two-dimensional junctions. For junctions without a ground plane, we conclude that step amplitudes on the order of 10 mA are practical, but significantly larger amplitudes require excessive microwave power.

[Contact: Richard L. Kautz, (303) 497-3391]

**Kautz, R.L., and Benz, S.P., Metallic-Barrier Junctions for Programmable Josephson Voltage Standards**, to be published in the Proceedings of the European Conference on Applied Superconductivity, Edinburgh, Scotland, July 3-7, 1995.

The current amplitudes of Shapiro steps are studied in large-area metallic-barrier Josephson junctions by simulation and experiment. Simulations show that junctions larger than about four times the Josephson penetration depth are of limited utility because the microwave power required to induce Shapiro steps increases exponentially with junction size. Experimentally, step amplitudes as large as 7 mA are observed in Nb-PdAu-Nb sandwich junctions.

[Contact: Richard L. Kautz, (303) 497-3391]

**Richter, C.A., Seiler, D.G., and Pellegrino, J.G., Quantum Conductance Fluctuations in a New Size-Scale Regime.**

[See [Compound Materials](#).]**FUNDAMENTAL ELECTRICAL MEASUREMENTS**

Recently Published

**Hamilton, C.A., and Burroughs, C.J., The Performance and Reliability of NIST 10-V Josephson Arrays**, IEEE Transactions on Instrumentation and Measurement, Vol. 44, No. 2, pp. 238-240 (April 1995). [Also published in the Digest of the 1994 Conference on Precision Electromagnetic Measurements, Boulder, Colorado, June 27–July 1, 1994, pp. 99-100.]

This paper reviews eight years of fabrication of 10-V Josephson array chips at NIST and the performance and reliability of these chips at 22 different standards laboratories. Failure mechanisms and statistical data on failure rates are presented for devices made with both Nb/Nb<sub>2</sub>O<sub>5</sub>/Pb and Nb/Al<sub>2</sub>O<sub>3</sub>/Nb junctions.

[Contact: Clark A. Hamilton, (303) 497-3740]

**Hamilton, C.A., Burroughs, C.J., and Kautz, R.L., Josephson D/A Converter with Fundamental Accuracy**, IEEE Transactions on Instrumentation and Measurement, Vol. 44, No. 2, pp. 223-225 (April 1995). [Also published in the Digest of the 1994 Conference on Precision Electromagnetic Measurements, Boulder, Colorado, June 27–July 1, 1994, pp. 271-272.]

A binary sequence of series arrays of shunted Josephson junctions is used to make a 14-bit D/A converter. With 13 bias lines, any step number in the range -8192 to +8192 -1.2  $V_{max}$  to +1.2  $V_{max}$  can be selected in the time required to stabilize the bias current (a few microseconds). The circuit is a fast accurate dc reference, and makes possible the digital synthesis of ac waveforms whose amplitudes derive directly from the internationally accepted definition of the volt.

[Contact: Clark A. Hamilton, (303) 497-3740]

**Lavine, C.F., Cage, M.E., and Elmquist, R.E., Spectroscopic Study of Quantized Breakdown Voltage States of the Quantum Hall Effect**, Journal of Research of the National Institute of Standards and Technology, Vol. 99, No. 6, pp. 757-764 (November-December 1994).

Quantized breakdown voltage states are observed in a second, wide, high-quality GaAs/AlGaAs sample made from another wafer, demonstrating that quantization of the longitudinal voltage drop along the sample is a general feature of the

quantum Hall effect in the breakdown regime. The voltage states are interpreted in a simple energy conservation model as occurring when electrons are excited to higher Landau levels and then return to the original level. A spectroscopic study of these dissipative voltage states reveals how well they are quantized. The statistical variations of the quantized voltages increase linearly with quantum number.

[Contact: Marvin E. Cage, (303) 497-4224]

Stenbakken, G.N., Steiner, R., Olsen, P.T., and Williams, E., **Methods for Aligning the NIST Watt-Balance**, Proceedings of the 1995 IEEE Instrumentation and Measurement Technology Conference, Waltham, Massachusetts, April 23-26, 1995, pp. 247-251.

The NIST watt-balance has been developed to explore the possibility of monitoring the stability of the mass standard by means of electrical quantum standards. The mass standard is the last basic standard that is kept as an artifact. The watt-balance uses a movable coil in a radial magnetic field to compare the mechanical energy required to lift a kilogram mass in earth's gravity with the electrical energy required to move the coil the same distance in a magnetic field. The electrical energy is monitored in terms of quantized Hall resistance and Josephson's junction voltage standards. The accuracy of this experiment depends on a large number of factors. Among them are the ability to align the apparatus so that the movable coil and magnet are coaxial and aligned to the local vertical. Misalignment of the coil and magnet result in forces and torques on the coil. The coil is suspended like a pendulum, so responds easily to these torques and horizontal forces. This paper describes a computer program that was written to calculate the shape of the magnetic field and the torques and forces on the movable coil that result from any misalignments. This information is being used to develop an alignment procedure that minimizes misalignments and the errors they cause. This program has enhanced our understanding of the cause of torques about the vertical axis on the coil and the dependence of this torque on the magnetic field gradient.

[Contact: Gerard N. Stenbakken, (301) 975-4226]

## SEMICONDUCTOR MICROELECTRONICS

## Silicon Materials

Released for Publication

Bagchi, S., Lee, J.D., Krause, S.J., and Roitman, P., **Effect of Implant Dose on Formation of Buried Oxide Si Islands in Low-Dose SIMOX**, to be published in the Proceedings of the 1995 IEEE SOI Conference, Tucson, Arizona, October 2-5, 1995.

Low-dose SIMOX (oxygen implant  $<1 \times 10^{18} \text{ cm}^{-2}$ ), with buried oxide layer thickness from 80 nm to 200 nm, has recently emerged as a possible SOI material that is similar to, but with certain advantages over, high-dose SIMOX (typically  $1 \times 10^{18} \text{ cm}^{-2}$ ), with BOX thicknesses of 350 nm to 400 nm. These advantages include reduced wafer cost, higher thermal conductivity, and possible improvements in device performance. There are still, however, important issues that remain on the microstructure of low-dose SIMOX that may affect its quality and performance. These issues include the presence of crystalline defects in the top Si layer and the presence of Si islands in the buried oxide which can severely degrade dielectric properties. While the reasons for crystalline defect formation have been recently determined, the mechanism of Si island formation in the BOX are still unclear. Such understanding could assist in improved processing for fabricating high-quality BOX layers in low-dose SIMOX. In this paper, we are reporting on the effect of implant dose on the microstructural changes found during Si island formation.

[Contact: Peter Roitman, (301) 975-2077]

Bagchi, S., Lee, J.D., Krause, S.J., and Roitman, P., **Mechanism of Defect Formation in Low-Dose Oxygen Implanted Silicon-On-Insulator Material**.

The defects and microstructure of low-dose ( $<0.7 \times 10^{18} \text{ cm}^{-2}$ ), oxygen-implanted silicon-on-insulator (SIMOX) material were investigated as a function of implant dose and annealing temperature by plan-view and cross-sectional transmission electron microscopy. The threading-dislocations in low-dose ( $0.2 \geq 65 \times 10^{18} \text{ cm}^{-2}$ ), annealed SIMOX originate from unfaulting of long ( $\sim 10 \mu\text{m}$ ), shallow ( $0.3 \mu\text{m}$ ), extrinsic stacking faults generated during the



ramping stage of annealing. As dose increases, the defect density is reduced, and the structure of the buried oxide layer evolves dramatically. It was found that there is a dose window which give a lower density and a continuous buried oxide with a reduced density of Si islands in the buried oxide. [Contact: Peter Roitman, (301) 975-2077]

### Compound Materials

#### Released for Publication

Richter, C.A., Seiler, D.G., and Pellegrino, J.G., **Quantum Conductance Fluctuations in a New Size-Scale Regime.**

We report the results of new experimental studies of "universal" conductance fluctuations in a variety of millimeter-sized GaAs/AlGaAs heterostructures. The ability to observe these mesoscopic fluctuations in traditionally macroscopic semiconductor devices is due to the enhanced sensitivity of our magnetic field modulation measurement technique which allows a coherent interference effect to be observed and studied in a new large size-scale regime.

[Contact: Curt A. Richter, (301) 975-2082]

### Compound Materials

#### Recently Published

Pellegrino, J.G., Richter, C.A., Dura, J.A., Amirtharaj, P.M., Qadri, S.B., and Roughani, B., **Buffer Layer-Modulation-Doped Field-Effect-Transistor Interactions in the  $\text{Al}_{0.33}\text{Ga}_{0.67}\text{As}/\text{GaAs}$  Superlattice System,** Journal of Vacuum Science and Technology A, Vol. 13, No. 3, pp. 787-791 (May/June 1995).

The correlation between the structural and transport properties for a series of high-quality modulation-doped field-effect-transistor (MODFET) structures was made for various growth temperatures. X-ray reflectivity, X-ray diffraction, and magnetotransport measurements were used to assess structural quality and transport parameters. Four samples with growth temperatures in the range 500 to 630 °C were examined. The results show a correlation exists between the measured electron mobility and the quality of the interface width, as measured from satellite peaks of the buffer layer. In addition, these

results show, for the first time to the best of our knowledge, that a direct correlation can be made between X-ray reflectivity structural measurements and the measured electron mobility of high-quality gallium-arsenide-based MODFETs. Both X-ray and transport results suggest a higher-quality structure was obtained at higher growth temperatures.

[Contact: Joseph G. Pellegrino, (301) 975-2123]

### Analysis and Characterization Techniques

#### Recently Published

Nahum, M., and Martinis, J.M., **Hot-Electron Microcalorimeters as High-Resolution X-Ray Detectors,** Applied Physics Letters, Vol. 66, No. 23, pp. 3203-3205 (5 June 1995).

[See Cryoelectronic Metrology.]

Thomson, R.E., and Moreland, J., **Development of High Conductive Cantilevers for Atomic Force Microscopy Point Contact Measurements,** Journal of Vacuum Science and Technology B, Vol. 13, No. 3, pp. 1123-1125 (May/June 1995).

Several techniques for improving the electrical conductivity of micromachined silicon cantilevers for atomic force microscopy point contact measurements were investigated. The techniques studied included sputtering or evaporating thin layers of gold, platinum or silver onto the lower surface of the cantilever to create a conducting metal layer, and doping the cantilevers with phosphorus. It was found that the lowest resistance contacts to a gold surface can be made by the metal-coated tips, which can make stable point contacts with resistances as low as 30  $\Omega$  at a tip-sample force of 15  $\mu\text{N}$ .

[Contact: Ruth E. Thompson, (303) 497-3141]

### Device Physics and Modeling

#### Released for Publication

Lowney, J.R., **Monte Carlo Simulation of Scanning Electron Microscope Signals for Lithographic Metrology.**

[See [Dimensional Metrology](#).]

## Device Physics and Modeling

### Recently Published

Sanborn, B.A., **Electron-Electron Interactions, Coupled Plasmon-Phonon Modes, and Mobility in n-Type GaAs**, Physical Review B, Vol. 51, No. 20, pp. 14 256-14 264 (12 May 1995).

This paper investigates the mobility of electrons scattering from the coupled system of electrons and longitudinal-optical (LO) phonons in n-type GaAs. The Boltzmann equation is solved exactly for low-electric fields by an iterative method, including electron-electron and electron-LO-phonon scattering dynamically screened in the random-phase approximation (RPA). The LO-phonon self-energy is treated in the plasmon-pole approximation. Scattering from ionized impurities screened in static RPA is calculated with phase-shift cross sections, and scattering from RPA screened deformation potential and piezoelectric acoustic phonons is included in the elastic approximation. The results show that dynamic screening and plasmon-phonon coupling significantly modify inelastic scattering at low temperature and densities. The effect on mobility is obscured by ionized impurity scattering in conventionally doped material, but should be important in modulation doped-structures. For uncompensated bulk n-type GaAs, the RPA phase-shift model for electron-impurity scattering gives lower drift mobilities than the standard Thomas-Fermi or Born calculations, which are high compared to experiment. Electron-electron scattering lowers the mobility further, giving improved agreement with experiment, though discrepancies persist at high donor concentrations ( $n > 10^{18} \text{ cm}^{-3}$ ). When impurities are ignored, inelastic scattering from the coupled electron-phonon system is the strongest scattering mechanism at 77 K for moderate doping. This result differs from the standard model, neglecting mode coupling and electron-electron scattering, which has the acoustic modes dominant in this regime.

[Contact: Barbara A. Sanborn, (301) 975-2062]

Sanborn, B.A., **Nonequilibrium Total-Dielectric-Function Approach to the Electron Boltzmann**

**Equation for Inelastic Scattering in Doped Polar Semiconductors**, Physical Review B, Vol. 51, No. 20, pp. 14 247-14 255 (15 May 1995).

This paper describes a simple and general method for deriving the inelastic collision term in the electron Boltzmann equation for scattering from a coupled electron-phonon system and applies the method to the case of doped polar semiconductors. In the Born approximation, the inelastic differential scattering rate  $W^{\text{inel}}$  can be expressed in terms of the nonequilibrium total dynamic dielectric function, which includes both electronic and lattice contributions. Within the random-phase approximation,  $W^{\text{inel}}$  separates into two components: an electron-electron interaction containing the nonequilibrium distribution function for excitations of the electron gas and a Fröhlich interaction including the phonon distribution function self-energy due to polarization of the electrons. Each of these two interactions is screened by only the electronic part of the total dielectric function, which contains the high-frequency dielectric constant, unlike commonly used expressions that contain the static dielectric constant. The detailed balance between plasmons and electron-hole pairs in steady state is used to eliminate the nonequilibrium plasmon distribution from the Boltzmann equation, resulting in a dynamically screened electron-electron collision term. The phonon self-energy modifies the longitudinal optical-phonon dispersion so that two hybrid normal modes contribute to the electron-phonon collision term.

[Contact: Barbara A. Sanborn, (301) 975-2062]

## Insulators and Interfaces

### Recently Published

Tobin, S.P., Tower, J.P., Norton, P.W., Chandler-Horowitz, D., Amirtharaj, P.M., Lopes, V.C., Duncan, W.M., Syllaios, A.J., Ard, C.K., Giles, N.C., Lee, J., Balasubramanian, R., Bollong, A.B., Steiner, T.W., Thewalt, M.L.W., Bowen, D.K., and Tanner, B.K., **A Comparison of Techniques for Nondestructive Composition Measurements in CdZnTe Substrates**, Journal of Electronic Materials, Vol. 24, No. 5, pp. 697-705 (1995).

We report an overview and a comparison of nondestructive optical techniques for determining

alloy composition  $x$  in  $\text{Cd}_{1-x}\text{Zn}_x\text{Te}$  substrates for HgCdTe epitaxy. The methods for single-point measurements include a new X-ray diffraction technique for precision lattice parameter measurements using a standard high-resolution diffractometer, room-temperature photoreflectance, and low-temperature photoluminescence. We compare measurements on the same set of samples by all three techniques. Comparisons of precision and accuracy, with a discussion of the strengths and weaknesses of different techniques, are presented. In addition, a new photoluminescence excitation technique for full-wafer imaging of composition variations is described.

[Contact: Deane Chandler-Horowitz, (301) 975-2084]

### Dimensional Metrology

Released for Publication

Lowney, J.R., **Monte Carlo Simulation of Scanning Electron Microscope Signals for Lithographic Metrology.**

Two computer codes for simulating the backscattered, transmitted, and secondary-electron signals from targets in a scanning electron microscope are described. The first code, MONSEL-II, has a model target consisting of three parallel lines on a three-layer substrate, while the second, MONSEL-III, has a model target consisting of a two-by-two array of finite lines on a three-layer substrate. Elastic electron scattering is determined by fits to the Mott cross section. Both plasmon-generated electrons and ionized valence electrons are included in the secondary production. An adjustable quantity called the residual energy loss rate is added to the formula of Joy and Luo to obtain the measured secondary yield. The codes show the effects of signal enhancement due to edge transmission, known as blooming, as well as signal reduction due to neighboring lines, known as the black-hole effect.

[Contact: Jeremiah R. Lowney, (301) 975-2048]

### Microfabrication Technology

Recently Published

Cavicchi, R.E., Suehle, J.S., Kreider, K.G., Gaitan, M., and Chaparala, P., **Fast Temperature Programmed Sensing for Micro-Hotplate Gas Sensors**, IEEE Electron Device Letters, Vol. 16, No. 6, pp. 286-288 (June 1995).

We describe an operating mode of a gas sensor that greatly enhances the capability of the device to determine the composition of a sensed gas. The device consists of a micromachined hotplate with integrated heater, heat distribution plate, electrical contact pads, and sensing film. The temperature-programmed sensing technique uses millisecond time-scale temperature changes to modify the rates for adsorption, desorption, and reaction of gases on the sensing surface during sensor operation. A repetitive train of temperature pulses produces a patterned conductance response that depends on the gas composition, as well as the temperature pulse width, amplitude, and specific sequence of pulses. Results are shown for the vapors of water, ethanol, methanol, formaldehyde, and acetone.

[Contact: John S. Suehle, (301) 975-2247]

### Plasma Processing

Released for Publication

Christophorou, L.G., Van Brunt, R.J., and Olthoff, J.K., **Fundamental Processes in Gas Discharges**, to be published in the Proceedings of the XIth International Conference on Gas Discharges and Their Applications, Tokyo, Japan, September 11-15, 1995.

Recent aspects of fundamental processes in gas discharges are discussed. These include the effect of internal energy excitation of atoms and molecules on their interactions with slow electrons, the effect of temperature on electron attachment and detachment processes, photodissociation of molecules and photodetachment of anions, and interactions involved in discharge byproduct formation and discharge diagnostics. Reference is also made to fundamental processes in gas discharge materials used in plasma processing.

[Contact: Richard J. Van Brunt, (301) 975-2425]

Hwang, H.H., Olthoff, J.K., Van Brunt, R.J., Radovanov, S.B., and Kushner, M.J., **Evidence for Inelastic Processes for  $\text{N}_3^+$  and  $\text{N}_4^+$  from**

### **Energy Distributions in He/N<sub>2</sub> rf Glow Discharges.**

The Ion Energy Distributions (IEDs) striking surfaces in radio frequency (rf) glow discharges are important in the context of plasma etching during the fabrication of microelectronics devices. In discharges sustained in molecular gases or multi-component gas mixtures, the shape of the IED and the relative magnitudes of the ion fluxes are sensitive to ion-molecule collisions which occur in the presheath and sheath. Ions which collisionlessly traverse the sheaths or suffer only elastic collisions arrive at the substrate with a measurably different IED than do ions which undergo inelastic collisions. In this article we present measurements and results from parametric calculations of IEDs incident on the grounded electrode of an rf glow discharge sustained in a He/N<sub>2</sub> gas mixture while using a Gaseous Electronics Conference Reference Cell (33.3 Pa, 13.56 MHz). We found that the shape of the IEDs for N<sub>3</sub><sup>+</sup> and N<sub>4</sub><sup>+</sup> provide evidence for inelastic ion-molecule reactions which have threshold energies of <5 eV.

[Contact: James K. Olthoff, (301) 975-2431]

Rao, M.V.V.S., Radovanov, S.B., Van Brunt, R.J., and Olthoff, J.K., **Kinetic Energy Distribution of Ions Produced from Townsend Discharges in Neon and Argon**, to be published in the Proceedings of the 1995 International Conference on Physics of Electronic and Atomic Collisions, Whistler, British Columbia, Canada, July 26–August 1, 1995.

Results are reported from measurements of the kinetic energy distributions of mass selected ions from diffuse, Townsend discharges in neon and argon at high electric field-to-gas density (E/N) ratios from  $3 \times 10^{-18}$  V m<sup>2</sup> to  $6 \times 10^{-18}$  V m<sup>2</sup>. The ion energies were measured using a cylindrical mirror analyzer coupled to a quadrupole mass spectrometer. The measured ion energy distributions are compared with predictions from solving the Boltzmann transport equation, assuming that symmetric resonant charge transfer is the dominant ion-neutral interaction. Results for Ne<sup>+</sup> in Ne show evidence of deviations from equilibrium. [Contact: Richard J. Van Brunt, (301) 975-2425]

Van Brunt, R.J., Olthoff, J.K., and Radovanov, S.B., **Influence of Electrode Material on Measured Ion Kinetic-Energy Distributions in Radio-Frequency Discharges**, to be published in the Proceedings of the 22nd International Conference on Phenomena in Ionized Gases, Hoboken, New Jersey, July 31–August 5, 1995.

Evidence is presented for a significant influence of electrode surface material and condition on the measurement of the kinetic energies of ions sampled from discharges through an orifice in the electrode. Significant differences in ion energy shifts and/or discrimination of low-energy ions are found using aluminum and stainless-steel electrodes in a radio-frequency discharge cell. It is argued that the observed differences in energy shifts may be attributable in part to differences in charging of oxide layers on the electrode surface around the sampling orifice.

[Contact: Richard J. Van Brunt, (301) 975-2425]

Van Brunt, R.J., Olthoff, J.K., and Radovanov, S.B., **Kinetic-Energy Distributions of Ions Sampled from Radio-Frequency Discharges in Helium, Nitrogen, and Oxygen**, to be published in the Proceedings of the XIth International Conference on Gas Discharges and Their Applications, Tokyo, Japan, September 11-15, 1995.

Mass-resolved ion kinetic-energy distributions are measured for radio-frequency (rf) discharges sustained in helium, nitrogen, and oxygen in a parallel-plate plasma reactor. The dominant ions for each of the gases are observed to be the parent ions He<sup>+</sup>, N<sub>2</sub><sup>+</sup>, and O<sub>2</sub><sup>+</sup>, respectively, over a wide range of pressures (1.3 to 67 Pa) with an applied rf voltage of 200 V. Ion kinetic-energy distributions at the grounded electrode were measured for these ions, as well as for less abundant ions, such as He<sub>2</sub><sup>+</sup>, N<sup>+</sup>, N<sub>2</sub>H<sup>+</sup>, N<sub>3</sub><sup>+</sup>, N<sub>4</sub><sup>+</sup>, O<sup>+</sup>, and O<sub>3</sub><sup>+</sup>.

[Contact: Richard J. Van Brunt, (301) 975-2425]

### Plasma Processing

#### Recently Published

Radovanov, S.B., Van Brunt, R.J., and Olthoff, J.K., **Ion Kinetics and Symmetric Charge-Transfer Collisions In Low-Current, Diffuse (Townsend) Discharges In Argon and Nitrogen**, Physical

Review E, Vol. 51, No. 6, pp. 6036-6046 (June 1995).

Translational kinetic-energy distributions of mass-selected ions have been measured in diffuse, low-current Townsend-type discharges at high electric field-to-gas density ratios ( $E/N$ ) in the range of  $1 \times 10^{-8}$  -  $2 \times 10^{-18}$   $\text{Vm}^2$  (1 to 20 kTd). The discharges were generated in Ar and  $\text{N}_2$  under uniform-field conditions and ion energies were measured using a cylindrical-mirror energy analyzer coupled to a quadrupole mass spectrometer. The mean ion energies determined from measured energy distributions of  $\text{Ar}^+$  in Ar and  $\text{N}_2^+$  in  $\text{N}_2$  are compared with the mean energies predicted from solutions of the Boltzmann transport equation based on the assumption that symmetric resonant charge transfer is the predominant ion-neutral interaction. The results for  $\text{Ar}^+$  and  $\text{N}_2^+$  are consistent with predictions made using a constant (energy independent) cross section for which an effective ion temperature can be defined. However, for both ions, the measured mean energies tend to fall increasingly below the predicted values as  $E/N$  increases. The possible causes and significance of the differences between the measured and calculated mean ion energies are examined by considering collisions other than charge-transfer that can affect ion energies as well as uncertainties in the charge-transfer cross sections used in the calculations. Measurements were also made of the relative contributions from  $\text{N}^+$  and  $\text{Ar}^{2+}$  to the ion flux. Over the  $E/N$  range of interest,  $\text{N}^+$  accounts for less than 15% of the ion flux in nitrogen and  $\text{Ar}^{2+}$  accounts for less than 5% of the ion flux in argon.

[Contact: Svetlana B. Radovanov, (301) 975-2436]

Radovanov, S.B., Dzierżęga, Roberts, J.R., and Olthoff, J.K., **Time-Resolved Balmer-Alpha Emission from Fast Hydrogen Atoms in Low Pressure, Radio-Frequency Discharges in Hydrogen**, Applied Physics Letters, Vol. 66, No. 20, pp. 2637-2639 (May 15, 1995).

Doppler-broadened  $\text{H}_\alpha$  emission (656.28 nm) detected from a 13.56 MHz, parallel-plate, radio-frequency discharge in hydrogen indicates the presence of fast excited H atoms throughout the discharge volume. Time and spatially resolved measurements of the Doppler-broadened emission

indicate that the fast H atoms are formed primarily at the surface of the powered electrode with kinetic energies exceeding 120 eV.

[Contact: Svetlana B. Radovanov, (301) 975-2436]

### Photodetectors

Released for Publication

Vayshenker, I., Yang, S., Li, X., and Scott, T.R., **Automated Measurements of Nonlinearity of Optical Fiber Power Meters**, to be published in the Proceedings of SPIE (The International Society for Optical Engineering, P.O. Box 10, Bellingham, Washington 98227-0010), International Symposium on Optical Science Engineering and Instrumentation, San Diego, California, July 9-14, 1995.

A system has been developed for measuring the nonlinearity of an optical power meter or detector at a wavelength of 1285 nm and with a dynamic range of more than 60 dB. This system uses fiber optics components and is designed to accommodate common optical power meters and optical detectors connectorized with low backreflection connectors such as FC/APC. The measurement system is based on the triplet superposition method in which the incident power is divided in two controllable paths and then recombined. Measurements are performed in sets of three at various optical powers over the dynamic range of the meter. The power meter is linear only if the sum of the individual powers is equal to the combined power. The system also measures the range discontinuity between neighboring power ranges of an optical power meter. An algorithm has been developed to treat both the nonlinearity and the range discontinuity in the same manner. As a result, the measurements yield a correction factor for any power in any range. The measurement system typically produces results which have standard deviations as low as 0.02%. The system can be also used at 1550 nm and over a 90 dB dynamic range by adding the proper laser source and a fixed attenuator to the existing system. This measurement system provides accurate determination of optical power meter or detector linearity; the characterized detectors then can be used for such applications as power and attenuation measurements.

[Contact: Igor Vayshenker, (303) 497-3394]

Yang, S., Vayshenker, I., Li, X., Zander, M., and Scott, T.R., **Optical Detector Nonlinearity: Simulation**, to be published as NIST Technical Note 1376.

A unified mathematical treatment has been developed for five commonly used measurement methods of optical detector nonlinearity, and a computer simulation was conducted to compare these methods for different measurement conditions and data processing options. The triplet and differential methods are shown to give overall best results, and third and fourth order polynomial representations of the measurement result will yield least total error for a common practical measurement system.

[Contact: Igor Vayshenker, (303) 497-3394]

### Reliability

#### Recently Published

Cole, E.I., Jr., Suehle, J.S., Peterson, K.A., Chaparala, P., Campbell, A.N., Snyder, E.S., and Pierce, D.G., **OBIC Analysis of Stressed, Thermally-Isolated Polysilicon Resistors**, Proceedings of the 1995 IEEE International Reliability Physics Proceedings, Las Vegas, Nevada, April 4-6, 1995, pp. 234-243.

High-gain Optical Beam Induced Current (OBIC) imaging has been used for the first time to examine the internal structure effects of electrical stress on thermally isolated polysilicon resistors. The resistors are examined over a wide range of current densities, producing Joule heating up to ~1200 °C. Throughout this current density range, the OBIC images indicate a clustering of dopant under dc stress and a more uniform distribution under ac conditions. The OBIC images also reveal areas that are precursors to catastrophic resistor failure. In addition to OBIC imaging, conventional electrical measurements were performed, examining the polysilicon resistance degradation and time-to-failure as a function of electrical stress. The electrical measurements shows a monotonic increase in polysilicon resistor lifetime with frequency (up to 2 kHz) when subjected to a bipolar ac stress. The enhanced lifetime was observed

even under high-temperature (from Joule heating) stress conditions previously reported to be electromigration-free. The dopant redistribution indicated by the OBIC imaging is consistent with an electromigration stress experienced by the polysilicon resistors. The implications for thermally isolated polysilicon resistor reliability are examined briefly.

[Contact: John S. Suehle, (301) 975-2247]

Prendergast, J., Suehle, J.S., Chaparala, P., Murphy, E., and Stephenson, M., **TDDB Characterization of Thin SiO<sub>2</sub> Films with Bimodal Failure Populations**, Proceedings of the 1995 IEEE International Reliability Physics Proceedings, Las Vegas, Nevada, April 4-6, 1995, pp. 124-130.

For many years, Time Dependent Dielectric Breakdown (TDDB) has been the subject of much controversy. Two different field dependencies have been observed, and several acceleration models have been suggested. Of the two most popular models, one predicts that the log  $t_{50\%}$  is proportional to the electric field while the other predicts that it is proportional to the reciprocal of the electrical field. This paper helps to explain the discrepancies in the electric field dependence observed and demonstrate distinct differences in the TDDB behavior between extrinsic and intrinsic dielectric breakdown.

The paper deals with the extensive characterization of a 20 nm oxide using multiple wafer fabrication lots. The data generated indicate that the intrinsic wearout properties of the oxide are best modeled by the E-model with a field-dependent activation energy ( $E_a$ ) and a constant field-acceleration factor. Of the three lots used in the characterization, one exhibited bimodal characteristics with a large extrinsic population. This allowed the investigation of the extrinsic distribution separately which exhibited a 1/E dependence and a field-dependent activation energy. The paper shows that using censored data for bimodal distributions results in the incorrect model (1/E) being used to predict intrinsic wearout. The paper also shows that in order to differentiate between the two models, sample sizes must be run to 100% failure to ensure that true intrinsic wearout has been observed. The characterization matrix used in the evaluation was

very comprehensive and indicates E-fields of 7 MV/cm and below must be used to determine the correct field acceleration model.

[Contact: John S. Suehle, (301) 975-2247]

## **SIGNAL ACQUISITION, PROCESSING, AND TRANSMISSION**

### DC and Low-Frequency Metrology

Released for Publication

Dziuba, R.F., **Automated Resistance Measurements at NIST**, to be published in the Proceedings of the 1995 National Conference of Standards Laboratories Workshop and Symposium, Dallas, Texas, July 16-20, 1995.

NIST provides a calibration service for dc standard resistors over 17 decades of resistance from  $10^{-4} \Omega$  to  $10^{12} \Omega$  using seven independent measurement systems. Four measurement systems are completely automated for calibrating resistors from 1  $\Omega$  to 1 M $\Omega$ . A fifth system for high-resistance measurements is semi-automated. Plans are underway to fully automate this system, along with the remaining two measurement systems. The primary consideration to automate a measurement system is to improve the quality of measurements, and not simply to relieve the operator from tedious repetitive measurements. This paper describes the extent and future plans of resistance measurement automation at NIST.

[Contact: Ronald F. Dziuba, (301) 975-4239]

Elmquist, R.E., **Progress on the Quantized Hall Resistance Recommended Intrinsic/Derived Standards Practice**, to be published in the Proceedings of the National 1995 Conference of Standards Laboratories Workshop and Symposium, Dallas, Texas, July 16-20, 1995.

The quantized Hall resistance (QHR) standard requires characterization tests which determine if and how a particular QHR device should be used as an intrinsic standard. The initial characterization at a qualified QHR laboratory would provide the following: 1) verification that the device resistance was approximately equal to that of other QHR devices under prescribed conditions, 2) assurance that the QHR device meets recognized quality

construction standards, 3) determination of the effect of temperature in the range below 1.5K, and 4) determination of the approximate magnetic flux density which must be applied to measure the QHR standard. The device could then be used as a standard in another laboratory, which would be expected to characterize the device using procedures which are given in the Recommended Intrinsic/Derived Standards Practice. Some of the laboratory procedures are described.

[Contact: Randolph E. Elmquist, (301) 975-6591]

Lipe, T.E., **A Re-Evaluation of the NIST Low-Frequency Standards for ac-dc Difference in the Voltage Range of 0.6 V to 100 V.**

A re-evaluation of the NIST standards of ac-dc difference was undertaken in an effort to reduce the calibration uncertainty offered by NIST for thermal voltage converters at frequencies below 100 Hz. This paper describes the measurements taken in support of this effort, as well as the devices used for the re-evaluation and the analysis of the uncertainty of the measurements. This re-evaluation of the NIST low-frequency standards will permit a significant reduction in uncertainty for ac-dc difference calibrations at 10 Hz in the voltage range from 0.6 V through 100 V.

[Contact: Thomas E. Lipe, (301) 975-4251]

### DC and Low-Frequency Metrology

Recently Published

Huang, D.X., Lipe, T.E., Kinard, J.R., and Childers, C.B., **AC-DC Difference Characteristics of High-Voltage Thermal Converters**, IEEE Transactions on Instrumentation and Measurement, Vol. 44, No. 2, pp. 387-390 (April 1995).

This paper describes a study of high-voltage thermal converters (HVTCs) at voltages above 100 V at frequencies up to 100 kHz. Techniques for the construction of HVTCs are described, and the effects of aging and dielectric loss on the resistor, changes in the timing sequence of ac-dc difference tests, relay dead-times, warm-up times, and level dependence are given.

[Contact: Thomas E. Lipe, (301) 975-4251]

Kinard, J.R., Huang, D.X., and Novotny, D.B.,

**Performance of Multilayer Thin-Film Multijunction Thermal Converters**, IEEE Transactions on Instrumentation, Vol. 44, No. 2, pp. 383-386 (April 1995). [Also published in the Proceedings of the Digest of the 1994 Conference on Precision Electromagnetic Measurements, Boulder, Colorado, June 27—July 1, 1994, pp. 407-408.]

New multilayer, thin-film multijunction thermal converters suitable as high-performance ac-dc transfer standards have been fabricated and studied at NIST. This paper describes their thermal and physical features and the materials chosen to improve performance. Performance data are given over a wide range of frequencies and conditions. [Contact: Joseph R. Kinard, (301) 975-4259]

Laug, O.B., **A 100 Ampere, 100 kHz Transconductor Amplifier**, Proceedings of the 1995 IEEE Instrumentation and Measurement Technology Conference, Waltham, Massachusetts, April 23-26, 1995, pp. 506-511.

A high-current, wide-band transconductance amplifier is described that provides an unprecedented level of output current at high frequencies with exceptional stability. It is capable of converting a signal voltage applied to its input into a ground-referenced output current up to 100 A rms over a frequency range from dc to 100 kHz with a usable frequency extending to 1 MHz. The amplifier has a 1000 W output capability,  $\pm 10$  V of compliance, and can deliver up to 400 A peak-to-peak of pulsed current. The amplifier design is based on the principle of paralleling a number of precision bipolar voltage-to-current converters. The design incorporates a unique ranging system controlled by opto-isolated switches, which permit a full-scale range from 5 to 100 A. The design considerations for maintaining wide bandwidth, high-output impedance, and unconditional stability for all loads are discussed.

[Contact: Owen B. Laug, (301) 975-2412]

Thompson, C.A., **Apparatus for Resistance Measurement of Short, Small-Diameter Conductors**, IEEE Transactions on Instrumentation and Measurement, Vol. 43, No. 4, pp. 675-677 (August 1994).

A system for determining the dc resistance of individual conductors  $2 \mu\text{m}$  in diameter and 0.5 to 1 in. length is described. The system uses a four-wire measurement, computerized data acquisition, and unique sample handling and contacting methods. To demonstrate system operation, data from measurements made on small-diameter copper wires are presented. These wires were first measured in long lengths on another system and then cut into short lengths and remeasured on this system. The results from these two measurement systems show that this system is an effective tool for determining the resistance per unit length of short, small-diameter conductors.

[Contact: Curtis A. Thompson, (303) 497-5206]

Waltrip, B.C., and Oldham, N.M., **Digital Impedance Bridge**, IEEE Transactions on Instrumentation and Measurement, Vol. 44, No. 2, pp. 436-439 (April 1995).

An impedance bridge that compares two-terminal standard inductors to characterized ac resistors in the frequency range of 10 Hz to 100 kHz is described. A dual-channel, digitally-synthesized source and sampling digital multimeter are used to generate and measure relevant bridge signals. A linear interpolation algorithm is used to autocalibrate the bridge to a 1 nF gas dielectric capacitor. An intercomparison of the new bridge with existing measurement standards conducted in the low audio frequency range shows agreement of 50 to 200 parts in  $10^6$  for inductors for 1 mH to 10 H.

[Contact: Bryan C. Waltrip, (303) 497-2438]

### Waveform Metrology

Released for Publication

Paulter, N.G., **Selecting a Short-Pulse Laser System for Photoconductive Generation of High-Speed Electrical Pulses**.

The selection of a short-pulse laser is important in electrical pulse metrology applications where the electrical pulses are generated photoconductively. Not only is the duration of the generated electrical pulse important, but so is the peak amplitude of that pulse. Insufficient pulse amplitude may cause excessive uncertainty in measurement results. An approximation is presented that can provide



guidelines to selecting the optimal short-pulse laser that is based on photoconductor, laser, and measurement system characteristics.  
[Contact: Nicholas G. Paulter, (301) 975-2405]

### Waveform Metrology

#### Recently Published

Paulter, N.G., Jr., N.G., **A Causal Regularizing Deconvolution Filter for Optimal Waveform Reconstruction**, IEEE Transactions on Instrumentation and Measurement, Vol. 43, No. 5, pp. 740-747 (October 1994).

A causal regularizing filter is described for selecting an optimal reconstruction of a signal from a deconvolution of its measured data and the measurement instrument's impulse response. Measurement noise and uncertainties in the instrument's response can cause the deconvolution (or inverse problem) to be ill-posed, thereby precluding accurate signal restoration. Nevertheless, close approximations to the signal may be obtained by using reconstruction techniques that alter the problem so that it becomes numerically solvable. A regularizing reconstruction technique is implemented that automatically selects the optimal reconstruction via an adjustable parameter and a specific stopping criterion, which is also described. Waveforms reconstructed using this filter do not exhibit large oscillations near transients as observed in other regularized reconstructions. Furthermore, convergence to the optimal solution is rapid.

[Contact: Nicholas G. Paulter, Jr., (303) 497-2405]

Jones, C.A., Kantor, Y., Grosvenor, J.H., and Janezic, M.D., **Stripline Resonator for Electromagnetic Measurements of Materials**, Proceedings of the Symposium on Materials and Processes for Wireless Communication, Boston, Massachusetts, November 15-16, 1994, pp. 35-48.

The Electromagnetic Properties of Materials Program at the National Institute of Standards and Technology is described, including an outline of the current goals of the project and details of measurement techniques being used at NIST for characterizing dielectric and magnetic materials of importance in wireless communications in the rf

spectrum of interest.

[Contact: Claude M. Weil, (303) 497-5305]

### Cryoelectronic Metrology

#### Released for Publication

Booi, P.A.A., and Benz, S.P., **Design of High-Frequency, High-Power Oscillators Using Josephson-Junction Arrays**, to be published in the Proceedings of the European Conference on Applied Superconductivity, Edinburgh, Scotland, July 3-7, 1995.

We analyze the limitations imposed by junction capacitance and the parasitic inductance, that is associated with shunt resistors, on the performance of Nb/Al-AIO<sub>x</sub>/Nb-junction-based array oscillators. Wide junctions are used that are in-situ deposited on top of PdAu resistor films (to minimize inductance) and are situated above Nb ground planes (to ensure uniform current injection). From the measured parasitics, the maximum power and frequency are inferred that can be obtained for critical-current densities  $J_c \leq 100 \text{ kA/cm}^2$ . These finds are illustrated with experimental results of 2,000-junction arrays having  $J_c \approx 10 \text{ kA/cm}^2$  that were found to couple  $\leq 0.7 \text{ mW}$  to a  $52 \Omega$  load in the range 180 to 300 GHz.

[Contact: Peter A. A. Booi, (303) 497-5910]

Grossman, E.N., **Lithographic Antenna for Submillimeter and Infrared Frequencies**.

A semi-tutorial review of lithographic feed antennas is presented with an emphasis on issues that become important at extremely high frequencies.

[Contact: Erich N. (303) 497-5102]

Kautz, R.L., **Shapiro Steps in Large-Area Metallic-Barrier Josephson Junctions**.

[See Fundamental Electrical Measurements.]

Larsen, B.H., and Benz, S.P., **Stable Phase Locking In a Two-Cell Ladder Array of Josephson Junctions**, Applied Physics Letters, Vol. 66, No. 23, pp. 3209-3211 (June 1995).

The stability of the periodic solution of the two-cell ladder array has been numerically investigated in

order to explore intrinsic phase-locking mechanisms relevant to arrays and stacked junction oscillators. In zero magnetic field, the periodic-in-phase solution of the system is neutrally stable. However, this solution is stable over a finite voltage range when an applied control exceeds a critical value. The dependence upon system parameters of the boundaries of the stable range and the critical control current is investigated. Finally, the influence of the control current on the microwave power in a typical range of stability is calculated.

[Contact: Samuel P. Benz, (303) 497-5258]

Roshko, A., Goodrich, L.F., Rudman, D.A., Moerman, R., and Vale, L.R., **Magnetic Flux Pinning in Epitaxial  $\text{YBa}_2\text{Cu}_3\text{O}_{7-\delta}$  Thin Films.**

The influence of microstructure on the critical density of laser-ablated  $\text{YBa}_2\text{Cu}_3\text{O}_{7-\delta}$  thin films has been examined. Scanning tunneling microscopy was used to examine the morphologies of  $\text{YBa}_2\text{Cu}_3\text{O}_{7-\delta}$  films, and the morphology data were then correlated with measurements of the critical current density. The films were found to grow by an island nucleation and growth mechanism. The critical current densities of the films are similar to those of films with screw dislocation growth, indicating that screw dislocation growth is not necessary for good pinning. Films with higher densities of island growth features were found to have higher critical current densities in applied magnetic field. This increase in pinning with increased island density indicates that there may be defects trapped in the regions between growth features which contribute to pinning.

[Contact: Alexana Roshko, (303) 497-5420]

### Cryoelectronic Metrology

#### Recently Published

Benz, S.P., and Booi, P.A.A., **High-Frequency Oscillators Using Phase-Locked Arrays of Josephson Junctions**, Proceedings of the IEEE International Frequency Control Symposium, Boston, Massachusetts, June 1-3, 1994, pp. 666-669.

We present a basic description of Josephson junctions and discuss their use as GHz and THz oscillators. The resistively shunted junction model

is used to calculate the available power, linewidth, and operating frequency of the oscillators. We discuss how phase-locked arrays of junctions are used to achieve higher power and narrower linewidth. Two experimental examples of phase-locked emission are shown: one from on-chip detection circuits at 150 GHz and one detected off-chip showing a 13 kHz linewidth at 88.8 GHz.

[Contact: Samuel P. Benz, (303) 497-5258]

Grossman, E.N., and Vale, L.R., **Heterodyne Mixing and Direct Detection in High Temperature Josephson Junctions**, Proceedings of the Fifth International Symposium on Space Terahertz Technology, Ann Arbor, Michigan, May 10-12, 1994, pp. 244-263.

We have examined various properties of the high-characteristic frequency of YBCO superconductor-normal-superconductor Josephson junctions that are important to their performance as low-noise THz frequency mixers. Without far-infrared laser illumination, the microwave frequency noise temperature of our lowest noise device shows good agreement with the predictions of the resistively shunted Josephson model in an applicable region of bias. It has a maximum noise temperature of  $36 \pm 4$  K at a physical temperature of 4 K. When illuminated with a 404 GHz far-IR laser local oscillator and a chopped 77 K blackbody signal, strong modulation of the 1 GHz Intermediate Frequency (IF) noise power is observed. However, certain features of the modulated IF power signal strongly suggest that a large fraction of it is not true heterodyne detection. The spurious component is probably due to direct detection of the broadband hot load/cold load signal. We believe that reliable measurement of heterodyne performance will require narrowband signal sources.

[Contact: Erich N. Grossman, (303) 497-5102]

Grossman, E.N., Vale, L.R., and Rudman, D.A., **Microwave Noise in High- $T_c$  Josephson Junctions**, Applied Physics Letters, Vol. 66, No. 13, pp. 1680-1682 (March 1995).

We have measured the noise of  $\text{YBa}_2\text{Cu}_3\text{O}_{7-\delta}$  superconductor-normal-superconductor junctions whose high normal-state resistances and characteristic frequencies make them suitable for THz frequency mixers. By directly measuring the 1

GHz power spectral density delivered to a low-noise 50  $\Omega$  radiometer system, the noise could be measured over a wide range of dc voltage and temperature, without complications due to  $1/f$  noise, and without invoking any specific model. At a physical temperature of 4 K, the lowest noise junction had an available noise temperature of  $31 \pm 2$  K, corresponding to an effective noise temperature of the normal resistance of 9 K. The effective noise temperature of the normal resistance is approximately equal to the physical temperature at high temperatures, but approaches a limiting value at low temperatures, implying an excess current noise of unknown origin.

[Contact: Erich N. Grossman, (303) 497-5102]

Nahum, M., and Martinis, J.M., **Hot-Electron Microcalorimeters as High-Resolution X-Ray Detectors**, Applied Physics Letters, Vol. 66, No. 23, pp. 3203-3205 (June 1995).

Measurements are presented on a novel microcalorimeter for the detection of X-rays. This detector uses a normal metal film deposited on a thin membrane to absorb X-ray photons. The subsequent temperature rise of the electrons is measured from the current-voltage characteristics of a normal-insulator-superconductor tunnel junction, where part of the absorber forms the normal electrode. A superconducting-quantum-interference-device is used as a low-noise high-bandwidth readout for the junction. We have measured an energy resolution of 22 eV full width at half-maximum and a time constant of 15  $\mu$ s for a detector operating at 80 mK and having a 0.5  $\mu$ m thick Au absorber with an area of 100 x 100  $\mu$ m<sup>2</sup>.

[Contact: Michael Nahum, (303) 497-5430]

Reintsema, C.D., Ono, R.H., Harvey, T.E., Missert, N., and Vale, L.R., **Mutual Phase Locking in Systems of High- $T_c$  Superconductor-Normal Metal-Superconductor Junctions**, Proceedings of SPIE (The International Society for Optical Engineering, P.O. Box 10, Bellingham, Washington 98227-0010), Superconductive Devices and Circuits, Vol. 2160, pp. 208-218 (1994).

We have investigated the interaction between high-critical temperature (high- $T_c$ ) superconductor-normal metal-superconductor step-edge junctions coupled through a non-superconducting feedback loop. We

have characterized the strength of the interaction as a function of frequency and temperature for both a circuit without a groundplane and an all high- $T_c$  multilayer circuit incorporating a superconducting groundplane. We observed relative locking strengths (the ratio of the measured locking current  $I_L$  to the junctions average critical current  $\bar{I}_c$ ) as large as  $I_L/\bar{I}_c = 9\%$  and peak-locking frequencies as high as 1.06 THz. The maximum temperature at which locking occurred was 35 K. An analysis of the temperature dependence of the locking current accounting for thermal fluctuations in the context of Johnson noise from resistive elements in the circuit agrees well with our experimental observations.

[Contact: Ronald H. Ono, (303) 497-3762]

### Antenna Metrology

Released for Publication

Francis, M.H., Newell, A.C., Grimm, K.R., Hoffman, J., and Schrank, H.E., **Comparison of Ultralow-Sidelobe Antenna Far-Field Patterns Using the Planar Near-Field Method and the Far-Field Method.**

The planar near-field measurement method is a proven technology for measuring ordinary antennas operating in the microwave region. The development of very low-sidelobe antennas raises the question whether this method can be used to measure accurately these antennas. Recently, scientists at several organizations showed that data taken and processed with the planar near-field methodology, including probe correction, can be used to accurately measure the sidelobes of very low-sidelobe antennas to levels of -55 dB to -60 dB relative to the main beam peak. Some of these results are highlighted. The test antenna for this study was a slotted-waveguide array whose low sidelobes were known. The near-field measurements were conducted at the NIST planar near-field facility.

[Contact: Michael H. Francis, (303) 497-5873]

### Antenna Metrology

Recently Published

Francis, M.H., Kremer, D.P., Jacobson, M.D., Fedor, L.S., Hazen, D.A., and Madsen, W.B., **A Dual-**

**Frequency Millimeter-Wave Radiometer Antenna for Airborne Remote Sensing of Atmosphere and Ocean**, Proceedings of the Antenna Measurement Techniques Association Symposium, Long Beach, California, October 3-7, 1994, pp. 3-9.

Accurate multiwavelength radiometric remote sensing of the ocean and the atmosphere from an aircraft requires antennas with the same beamwidth at the various frequencies of operation. Scientists at the National Oceanic and Atmospheric Administration designed an offset antenna with a pressure-compensating corrugated feed horn to meet this criterion. A specially designed fairing was incorporated into the antenna to optimize the aerodynamics and minimize the liquid buildup on the antenna surfaces. The antenna has two positions: the zenith (up) position and the nadir (down) position. The planar near-field facility at the National Institute of Standards and Technology was used to determine the far-field pattern of the antenna. The results show that the antenna beamwidths at 23.87 and 31.65 GHz are nearly the same as expected from the design criterion. This antenna was recently used in an ocean remote-sensing experiment and performed according to expectations.

[Contact: Michael H. Francis, (303) 497-5873]

Guerrieri, J.R., and Tamura, D.T., **Effects of Microwave Absorber on Insertion-Loss Measurements**, Proceedings of the Antenna Measurement Techniques Association Symposium, Long Beach, California, October 3-7, 1994, pp. 221-229.

Absorber material is used in antenna measurements to reduce multiple reflections and multipath. However, in some cases this absorber can still have an uncertainty larger than the desired uncertainty of the measurement.

For accurate antenna gain measurements, using the planar, cylindrical, and spherical near-field methods, insertion loss measurements should be accurate to within +0.03 dB. To satisfy this requirement, it is important to minimize the multiple reflections between the probe and antenna under test. If the multiple reflections are too large, then the insertion loss becomes very position sensitive, and errors on

the order of a decibel can be introduced. It is imperative that absorber be used to cover all metal surfaces. Errors can also be introduced if the absorber is not used carefully. The effects on antenna gain data measured with and without absorber are shown. Measurement results showing the effect of the placement of the absorber on the antenna under test are also presented. This includes absorber distance from the antenna's aperture, the rotation of absorber about the antenna's coordinate system, and the use of different types of absorber.

[Contact: Jeff Guerrieri, (303) 497-3863]

#### Microwave and Millimeter-Wave Metrology

##### Released for Publication

Clague, F.R., **A Calibration Service for Coaxial Reference Standards for Microwave Power**, to be published as NIST Technical Note 1374.

A calibration service at NIST for coaxial microwave power reference standards is described. The service provides measurements of the reference standard effective efficiency from 50 MHz to 18 GHz at a power level of 10 mW. In the Report of Calibration, the effective efficiency is reported in percent. The NIST microwave power standards consists of both a microcalorimeter and an associated reference standard. The reference standard is a bolometric-type power detector (a thermistor mount). The only thermistor mounts accepted for measurement are those constructed to NIST specifications which are compatible with the coaxial microcalorimeter. These thermistor mounts and the automated microcalorimeter are described. A detailed error analysis with an estimate of the calibration uncertainties and their sources is included. The calibration uncertainty, which is quoted as a function of frequency, ranges from about 0.2% at 50 MHz to 0.4% at 18 GHz.

[Contact: Fred R. Clague, (303) 497-5778]

#### Microwave and Millimeter-Wave Metrology

##### Recently Published

Hayden, L.A., and Marks, R.B., **Accuracy in Time Domain Transmission Line Measurements**, Proceedings of the IEEE 3rd Topical Meeting on

Electrical Performance of Electronic Packaging, Monterey, California, November 2-4, 1994, pp. 176-178.

This paper examines time domain methods for characterizing signal propagation in uniform transmission lines. The impact of the limitations associated with time domain instrumentation and methodologies are examined, and guidelines for minimizing errors are presented.

[Contact: Leonard A. Hayden, (303) 497-3400]

Marks, R.B., and Williams, D.F., **Comments on "Conversions Between S, Z, Y, h, ABCD, and T Parameters Which Are Valid for Complex Source and Load Impedance,"** IEEE Transactions on Microwave Theory and Techniques, Vol. 43, No. 4, pp. 914-915 (April 1995).

A recently published paper [D.A. Frickey, IEEE Trans. Microwave Theory Tech., Vol. 42, pp. 205-211, Feb. 1994], presents formulas for conversions between various network matrices. However, these parameters are defined using an unconventional definition of the waves and therefore yield unexpected results.

[Contact: Roger B. Marks, (303) 497-3037]

Williams, D.F., and Marks, R.B., **LRM Probe-Tip Calibrations Using Nonideal Standards,** IEEE Transactions on Microwave Theory and Techniques, Vol. 43, No. 2, pp. 466-469 (February 1995).

The line-reflect-match calibration is enhanced to accommodate imperfect match standards and lossy lines typical of monolithic microwave integrated circuits. We characterize the match and line standards using an additional line standard of moderate length. The new method provides a practical means of obtaining accurate, wideband calibrations with compact standard sets. Without the enhancement, calibration errors due to imperfections in typical standards can be severe.

[Contact: Dylan F. Williams, (303) 497-3138]

### Electromagnetic Properties

Released for Publication

Baker-Jarvis, J.R., and Jones, C.A., **Dielectric Measurements on Printed-Wiring and Circuit Boards, Thin Films, and Substrates: An Overview,** to be published in the Proceedings of the Materials Research Society, San Francisco, California, April 18, 1995.

A review of the most common methods of permittivity measurements for thin films, printed-wiring boards, circuit boards, and substrates is presented. Transmission-line techniques, coaxial apertures, open-resonators, surface-wave modes, and dielectric resonators methods are examined. The frequency range of applicability and typical uncertainties associated with each method are summarized.

[Contact: James R. Baker-Jarvis, (303) 497-5621]

Baker-Jarvis, J.R., Jones, C.A., Riddle, B.F., Janezic, M.D., Geyer, R.G., Grosvenor, J.H., Jr., and Weil, C.M., **Survey of Nondestructive and Process Control Dielectric and Magnetic Measurements.**

A review of the most common methods for nondestructive permittivity and measurements is presented. Transmission line techniques, coaxial apertures, open-resonators, surface-wave modes, and dielectric resonators methods are examined. Measurements on bulk and thin materials and thin films are addressed. Measurement fixtures then can be operated as sensors are highlighted. The frequency range of applicability and typical uncertainties associated with each method are addressed.

[Contact; James R. Baker-Jarvis, (303) 497-5621]

Ceremuga, J., Krupka, J., Geyer, R.G., and Modelski, J., **Influence of Film Thickness and Air Gaps in Surface Impedance Measurements of High Temperature Superconductors Using the Dielectric Resonator Technique.**

The sapphire dielectric resonator technique is commonly used for microwave surface resistance measurements of high-temperature superconducting (HTS) films. So far, the impact of HTS film thickness on measurement results has not been taken into account. A theoretical mode-matched solution analysis of  $TE_{011}$  10 GHz sapphire dielectric resonator was performed. The results of this

analysis demonstrate that the thickness of the superconducting film under test can significantly affect both the resonant frequency ( $f_{res}$ ) and quality factor (Q) of the resonant system, particularly when the thickness is less than 3 times the London penetration depth ( $\lambda$ ) of the film at the operating temperature. In such cases, the microwave properties of the substrate affect  $f_{res}$  and Q. For HTS film thickness small relative to  $\lambda$ , measured quality factor and resonant frequency may also be affected by substrate thickness and the conductivity of the backing plates of the system. The presence of air gaps between the sapphire resonator and the HTA films does not significantly influence surface-resistance measurements. However, they can markedly affect the surface reactance, from which the penetration depth is calculated.

[Contact: Richard G. Geyer, (303) 497-5533]

Jones, C.A., Kantor, Y., Grosvenor, J.H., and Janezic, M.D., **Stripline Resonator for Electromagnetic Measurement of Materials.**

A stripline resonator was used to measure the relative dielectric and magnetic properties of materials in the frequency range from 150 MHz to 2 GHz. Measurement accuracy relates strongly to the dimensions of the resonator; therefore, equations used in the design of a resonator and the design of the resonator is described along with the major advantages and disadvantages. Dielectric and magnetic measurements are included to support the design of our resonator. Discussions of important concepts used in measurement correction, such as sample shape and size and demagnetization, are provided.

[Contact: Chriss A. Jones, (303) 497-5958]

Krupka, J., and Geyer, R.G., **Complex Permeability of Demagnetized Microwave Ferrites Near and Above Gyromagnetic Resonance.**

A wide variety of microwave ferrite phase-shifting materials has been measured in the demagnetized state. The relative magnetic permeability and loss factor were determined near and above natural gyromagnetic resonance using  $H_{011}$  cylindrical dielectric ring resonators. These low-loss dielectric sleeves were dimensioned for accurate magnetic

property measurements of single ferrite rod samples at logarithmically sampled resonant frequencies from 2 GHz to 25 GHz. Permeability and magnetic loss factor are computed from the measured resonant frequencies and Q factors of these resonators with and without the ferrite sample using exact eigenvalue equations. Generally, the real part of the complex magnetic permeability increases with decreasing saturation magnetization, while the magnetic loss factor increases nonlinearly with increasing saturation. Although Schloemann's theoretical model of the permeability of a cylinder in the completely demagnetized state is a first approximation, measured results differ from theoretical predictions. The data allow design optimization of circulators, isolators, and dual-mode and polarization-insensitive phasers, which are widely used in antenna array systems.

[Contact: Richard G. Geyer, (303) 497-5533]

Randa, J.P., **A Low-Frequency Model for Radio-Frequency Absorber**, to be published in the Journal of Research of the National Institute of Standards and Technology.

A simple model is developed to characterize the behavior of radio-frequency absorber at low frequency. The absorber is represented by a flat, homogeneous, isotropic slab of lossy material, with effective constitutive parameters. These parameters are determined by a fit to measured data. Excellent fits are obtained in the two applications considered. The model is intended for use in the characterization of absorber-lined chambers at low frequency. It could also be used to predict the low-frequency performance of partially loaded shielded enclosures.

[Contact: James P. Randa, (303) 497-3150]

### Electromagnetic Properties

#### Recently Published

Geyer, R.G., and Krupka, J., **Microwave Dielectric Properties of Anisotropic Materials at Cryogenic Temperatures**, IEEE Transactions on Instrumentation and Measurement, Vol. 44, No. 2, pp. 329-331 (April 1995).

The permittivity and dielectric loss tangent of cross-linked polystyrene (Rexolite), polytetrafluoroethylene

(Teflon), and single-crystal quartz were measured at microwave frequencies and at temperatures of 77 K and 300 K using a dielectric resonator technique. Dielectric loss tangents as low as  $7 \times 10^{-6}$  at 77 K were determined by applying high-temperature superconducting (HTS) films as the endplates of the dielectric resonator. Two permittivity tensor components for uniaxially anisotropic crystalline quartz were measured. Although the permittivities at 77 K changed very little from their room temperature values at 300 K, large changes in dielectric losses were observed. The decreased loss characteristics of these microelectronic substrates can markedly improve the performance of many microwave devices at cryogenic temperatures.

[Contact: Richard G. Geyer, (303) 497-5852]

### Laser Metrology

Released for Publication

Rochford, K.B., and Rose, A.H., **Simultaneous Laser Diode Emission and Detection for Fiber Optic Sensor Applications.**

The simultaneous emission and detection of radiation with a semiconductor laser is investigated. Measured signal-to-noise ratios of up to 56 dB demonstrate that these devices are adequate for sensor applications with discrete measurands. A strong polarization dependence which can cause response fluctuations is reported, and methods to minimize this fluctuation are discussed. This technique could be used for lower-cost sensors without splitters and detectors.

[Contact: Kenneth B. Rochford, (303) 497-5170]

Zhang, Z.M., Livigni, D., Jones, R.D., and Scott, T.R., **Thermal Modeling and Analysis of Laser Calorimeters.**

We have performed a detailed thermal analysis and modeling of the C-series laser calorimeters available at NIST for calibrating laser power or energy meters. A finite-element method was employed to simulate the space and time dependence of temperature at the calorimeter receiver. The nonequivalence due to different spatial distributions of the heating power was

investigated: The nonequivalence between the front heater and the rear heater was found to be  $\approx 1.7\%$ , and the nonequivalence between the laser and the rear heater was estimated to be  $<0.05\%$ . The computational results are in good agreement with experiments at the 1% level. The effects of the deposited energy, power duration, and relaxation time on the calibration factor and cooling constant were investigated. This paper presents a comprehensive thermal evaluation of the C4 calorimeters and provides information for future design improvement.

[Contact: David J. Livigni, (303) 497-5898]

### Laser Metrology

Recently Published

Jones, R.D., and Scott, T.R., **Characterization of a Clipped Gaussian Beam**, Proceedings of SPIE (The International Society for Optical Engineering, P.O. Box 10, Bellingham, Washington 98227-0010), Beam Control, Diagnostics, Standards, and Propagation, Vol. 2375, pp. 360-374 (1995).

We calculated irradiance distributions resulting from clipping a Gaussian beam with hard-edged slits transmitting 99 or 95% of the incident power. We determined the widths -- second moment (with 8- and 12-bit resolution), scanning slit, and knife-edge -- of these profiles at several distances from the source, both with and without a focusing lens. When using a lens, we had the option of determining the characterization parameters from two beam width measurements and one axial distance, or from a least-squares fit of several beam width measurements and axial distances. Characterization parameters determined by these two options can differ significantly, and under the conditions of this study, beam divergence is more accurately determined from a single beam width measurement than from a least-squares fit of several measurements. Finite resolution of irradiance, inherent in any measurement device, truncates integrals necessary for calculation of the second moment of irradiance distributions.

[Contact: Richard D. Jones, (303) 497-3439]

### Optical Fiber Metrology

Released for Publication

Mechels, S.E., and Franzen, D.L., **Accurate Measurements of Zero-Dispersion Wavelength in Single-Mode Fibers**, to be published in the Proceedings of the 3rd Optical Fibre Measurement Conference (OFMC '95), Liège, Belgium, September 25-26, 1995.

A highly accurate frequency-domain phase shift system for measuring the zero dispersion wavelength ( $\lambda_0$ ) of optical fibers has been developed. For 5 to 10 km fibers,  $\lambda_0$  can be determined with a precision of  $\pm 0.1$  nm or less (three standard deviations); possible sources of systematic error have been identified. The system has been used to study the long-term behavior of  $\lambda_0$  measurements and fibers evaluated for their suitability as standard reference fibers.

[Contact: Steven E. Mechels, (303) 497-5409]

Mechels, S.E., Schlager, J.B., and Franzen, D.L., **Accurate Zero-Dispersion Wavelength Measurements in Single-Mode Fibers: Two Frequency-Domain Methods**, to be published in the Proceedings of the IEEE Lasers and Electro-Optics 1995 Annual Meeting, (LEOS '95), San Francisco, California, October 30–November 2, 1995.

Two dispersion measurement systems are compared based on the frequency-domain phase shift and differential-phase shift techniques. Both systems are capable of measuring the zero-dispersion wavelength ( $\lambda_0$ ) in optical fiber with precisions of  $\pm 0.1$  nm; however, their accuracies have yet to be determined. By comparing the two systems, an estimate is obtained on the size of potential systematic errors. At this point, accuracies on the order of 0.2 to 0.3 nm can be claimed. The experimental apparatus is briefly described, and the measurement results are compared. Some possible sources of systematic error are mentioned. The systems will be used to characterize  $\lambda_0$  in standard reference fibers.

[Contact: Steven E. Mechels, (301) 497-5409]

Rochford, K.B., and Rose, A.H., **Simultaneous Laser Diode Emission and Detection for Fiber Optic Sensor Applications**.

[See Laser Metrology.]

Williams, P.A., and Hernday, P.R., **Experimental Observation of Anomalous Relation between Time and Frequency Domain PMD Measurements**, to be published in the Proceedings of the 3rd Optical Fibre Measurement Conference (OFMC '95), Liège, Belgium, September 25-26, 1995.

Nearly simultaneous measurements are reported of Polarization Mode Dispersion (PMD) in various samples of single-mode fiber using the measurement methods of Jones Matrix Eigenanalysis (JME) and Fourier transformed wavelength scanning (WSFT). It is shown that the ratio of the PMD values resulting from these two methods differs by approximately 10% from current theoretical predictions. The measurement methods are verified by demonstrating the theoretical agreement between JME and Wavelength Scanning Extrema Counting results.

[Contact: Paul A. Williams, (303) 497-3805]

Williams, D.H., Young, M., and Tietz, L.A., **Fiber Coating Diameter: Toward a Glass Artifact Standard**, to be published in the Proceedings of the 3rd Optical Fibre Measurement Conference (OFMC '95), Liège, Belgium, September 25-26, 1995.

The development of a glass standard for the calibration of outer primary coating diameter measurements is discussed. The proposed standard is a glass fiber, 250  $\mu\text{m}$  in diameter, with an index of refraction similar to that of the coating. The method of manufacturing the glass fiber, the refractive index measurements, and the contact diameter measurements are presented in this report.

[Contact: Matt Young, (303) 497-3223]

#### Optical Fiber/Waveguide Sensors

Released for Publication

Patrick, H., and Gilbert, S.L., **Comparison of UV Photosensitivity and Fluorescence During Fiber Grating Formation**, to be published in the Proceedings of the Photosensitivity and Quadratic Nonlinearity in Glass Waveguides: Fundamentals and Applications Topical Meeting, Portland, Oregon, September 9-11, 1995.



In this paper, it is shown that the ultraviolet photosensitivity of optical fiber is strongly correlated with the amount of change in the blue fluorescence emitted during the exposure.

[Contact: Heather Patrick, (303) 497-6353]

### Integrated Optics

#### Released for Publication

Christensen, D.H., McCollum, M.J., Hill, J.R., and Rai, R.S., **Variations from Periodicity in Distributed Bragg Reflectors**, to be published in the Proceedings of the IEEE Conference on Lasers and Electro-Optics, Baltimore, Maryland, May 21-26, 1995.

Systematic and random variations in layer thickness throughout semiconductor Bragg reflectors are investigated. They are characterized using transmission electron microscopy, double-crystal X-ray diffractometry, reflectance spectroscopy, rocking curve simulations, and reflectance simulations.

[Contact: David H. Christensen, (303) 497-3354]

### Integrated Optics

#### Recently Published

Grossman, E.N., and McDonald, D.G., **Partially Coherent Transmittance of Dielectric Lamellae**, Optical Engineering, Vol. 34, No. 5, pp. 1289-1295 (May 1995).

We derive an analytic formula for the transmittance of a dielectric lamella when the interference between successive internal reflections is only partially spatially coherent. This allows effects such as surface roughness and non-parallelism, which produce cumulative distortions in the phasefront with each reflection and which result in a loss of fringe contrast at high frequencies, to be accounted for quantitatively. The transmittance of a Si lamella, measured with a Fourier-transform interferometer over the range 20 to 1000  $\text{cm}^{-1}$ , agrees with our formula to within the accuracy of the data, which is dominated by systematic instrumental effects.

[Contact: Erich N. Grossman, (303) 497-5102]

### Complex System Testing

#### Recently Published

Stenbakken, G.N., **Effects of Nonmodel Errors on Model-Based Testing**, Proceedings of the 1995 IEEE Instrumentation and Measurement Technology Conference, Waltham, Massachusetts, April 24-26, 1995, pp. 38-42.

In previous work, methods have been developed for efficient testing of components and instruments that are based on models of these units. These methods allow for the full behavior of these units to be predicted from a small but efficient set of test measurements. Such methods can significantly reduce the testing cost of such units by reducing the amount of testing required. These methods are valid only as long as the model accurately represents the behavior of the units. Previous papers on this subject described many methods for developing accurate models and using them to develop efficient test methods. However, they gave little consideration to the problem of testing units which change their behavior after the model has been developed, for example, as a result of changes in the manufacturing process. Such changed behavior is referred to as nonmodel behavior or nonmodel error. When units with this new behavior are tested with these more efficient methods, their predicted behavior can show significant deviations from their true behavior. This paper describes how to analyze the data taken at the reduced set of measurements to estimate the uncertainty in the model predictions, even when the device has significant nonmodel error. Results of simulation are used to verify the accuracy of the estimates and to show the expected variation in the results for many modeling variables.

[Contact: Gerald N. Stenbakken, (301) 975-2440]

### Other Signal Topics

#### Released for Publication

Kautz, R.L., **CHAOS**.

Since the time of Newton, the science of dynamics has provided quantitative descriptions of regular motion, from a pendulum's swing to a planet's orbit, expressed in terms of differential equations. However, the role of Newtonian mechanics has recently expanded with the realization that it can

also describe chaotic motion. In elementary terms, chaos can be defined as pseudorandom behavior observed in the steady-state dynamics of a deterministic nonlinear system. How can motion be pseudorandom, or random, according to statistical tests, and yet be entirely predictable? This is just one of the paradoxes of chaotic motion, which is also globally stable but locally unstable, predictable in principle but not in practice, and geometrically complex but derived from simple equations.

[Contact: Richard L. Kautz, (303) 497-3391]

### Other Signal Topics

#### Recently Published

Deyst, J.P., and Souders, T.M., **Bounds on Frequency Response Estimates Derived from Uncertain Step Response Data**, Proceedings of the 1995 IEEE Instrumentation and Measurement Technology Conference, Waltham, Massachusetts, April 24-26, 1995, pp. 252-257.

A system's frequency response can be estimated from measurements of its step response; however, many error sources affect the accuracy of such estimates. This paper investigates the effects of uncertainty in the knowledge of the step response. Methods for establishing uncertainty bounds for the frequency response estimates are developed, based on the corresponding time-domain uncertainties associated with the step-like waveform. Two methods are described. One is a provable upper bound that is often very conservative. The other is more realistic, but it is based on an unproved conjecture. End effects that influence the bounds are also considered. A simulated example of the bounds is presented.

[Contact: John P. Deyst, (301) 975-2437]

Deyst, J.P., Souders, T.M., and Solomon, O.M., **Bounds on Least-Squares Four-Parameter Sine-Fit Errors**, IEEE Transactions on Instrumentation and Measurement, Vol. 44, No. 3, pp. 637-642 (June 1995).

Least-squares sine-fit algorithms are used extensively in signal processing applications. The parameter estimates produced by such algorithms are subject to both random and systematic errors when the record of input samples consists of a

fundamental sine wave corrupted by harmonic distortion or noise. The errors occur because in general, such sine-fits will incorporate a portion of the harmonic distortion or noise into their estimate of the fundamental. Bounds are developed for these errors for least-squares four-parameter (amplitude, frequency, phase, and offset) sine-fit algorithms. The errors are functions of the number of periods in the record, the number of samples in the record, the harmonic order, and fundamental and harmonic amplitudes and phases. The bounds do not apply to cases in which harmonic components become aliased.

[Contact: John P. Deyst, (301) 975-2437]

Reeve, G.R., and Friday, D.S., **NIST and the Navy - Past, Present and Future**, Proceedings of the Test and Calibration Symposium, American Society of Naval Engineers, Washington, DC, November 30—December 1, 1994, pp. 229-237.

The National Institute of Standards and Technology, formerly known as the National Bureau of Standards, founded in 1901, has had an historic and fruitful relationship with the Department of Defense, its predecessors, and the three military services, particularly the Navy. In this paper we outline some of the historic support, current collaborations, and what areas of technology may require our support for the Navy of the future.

[Contact: Jerome R. Reeve, (303) 497-3557]

Young, M., **Comment on Etalon Effects in Laser Mirrors**, Optical Engineering, Vol. 34, No. 4, p. 1243 (April 1995).

This note points out that the transmittance of a Fabry-Perot interferometer that has mirrors with unequal reflectances can be calculated with the usual formula, provided that  $R$  and  $T$  are replaced by the geometric means.

[Contact: Matt Young, (303) 497-3223]

## **ELECTRICAL SYSTEMS**

### Power Systems Metrology

Released for Publication

Christophorou, L.G., **Electron Attachment to Excited Molecules**, to be published in the

Proceedings of the International Symposium on Electron- and Photon-Molecule Collisions and Swarms, Berkeley, California, July 22-25, 1995.

The interactions of slow electrons with molecules, especially the processes of electron attachment, depend rather strongly on the internal energy content of the molecules themselves. As a rule, excited molecules interact with slow electrons with substantially larger cross sections than do ground-state molecules. Studies of electron attachment to vibrationally/rotationally excited, "hot," molecules and especially to electronically excited molecules are rather recent, in contrast to the extensive studies on electron attachment to ground-state molecules which cover many decades. Recent studies on electron attachment to thermally excited (or infrared-laser-excited vibrationally/rotationally excited) molecules showed that the effect of internal energy of a molecule on its electron attachment properties depends on the mode, dissociative or nondissociative, of electron attachment; and recent studies of electron attachment to electronically excited molecules, especially photoenhanced dissociative electron attachment to short- and long-lived excited electronic states of molecules produced directly or indirectly by laser irradiation, are discussed.

[Contact: Loucas G. Christophorou, (301) 975-2432]

Huecker, T., von Glahn, P., Kranz, H.G., and Okamoto, T., **A Standardized Computer Data File Format for Storage, Transport, and Off-Line Processing of Partial Discharge Data**, to be published in the Proceedings of the 9th International Symposium of High-Voltage Engineering, Graz, Austria, August 28–September 1, 1995.

An overview of a proposed data file format for digitized partial discharge data is presented. The proposed format will permit investigators at different institutions to exchange PD data and collaborate on the analysis and understanding of the PD phenomenon. An example is included in which investigators at all three institutions evaluated the same data record and report their analysis results.

[Contact: Peter von Glahn, (301) 975-2427]

Martzloff, F.D., **Keeping Up with the Reality of**

**Today's Surge Environment**, to be published in the Proceedings of the 1995 Power Quality/Mass Transit Conference, Ventura, California, September 11-15, 1995.

The paper proposes to establish a program for characterizing surge events by the capacity of a surge event to deliver a surge current through the power system in end-user facilities. This measurement would complement or even supersede the conventional monitoring of surge voltages. Two approaches are proposed: (1) using a metal-oxide varistor with the lowest possible voltage to "attract" surges away from other SPDs connected in the facility, and then recording the surge current waveform in the varistor; and (2) gathering data on field failures attributable to surges or swells of all types of electrical appliances and then attempting to replicate the failure mode in the laboratory.

[Contact: François D. Martzloff, (301) 975-2409]

Rao, M.V.V.S., Radovanov, S.B., Van Brunt, R.J., and Olthoff, J.K., **Kinetic Energy Distribution of Ions Produced from Townsend Discharges in Neon and Argon**, to be published in the Proceedings of the 1995 International Conference on Physics of Electronic and Atomic Collisions, Whistler, British Columbia, Canada, July 26–August 1, 1995.

Results are reported from measurements of the kinetic energy distributions of mass selected ions from diffuse, Townsend discharges in neon and argon at high electric field-to-gas density ( $E/N$ ) ratios from  $3 \times 10^{-18} \text{ V m}^2$  to  $6 \times 10^{-18} \text{ V m}^2$ . The ion energies were measured using a cylindrical mirror analyzer coupled to a quadrupole mass spectrometer. The measured ion energy distributions are compared with predictions from solving the Boltzmann transport equation, assuming that symmetric resonant charge transfer is the dominant ion-neutral interaction. Results for  $\text{Ne}^+$  in Ne show evidence of deviations from equilibrium.

[Contact: Richard J. Van Brunt, (301) 975-2425]

Van Brunt, R.J., Olthoff, J.K., Firebaugh, S.L., and Sauers, I., **Measurement of  $\text{S}_2\text{F}_{10}$ ,  $\text{S}_2\text{OF}_{10}$ , and  $\text{S}_2\text{O}_2\text{F}_{10}$  Production Rates from Spark and Negative Glow Corona Discharge in  $\text{SF}_6/\text{O}_2$  Gas Mixtures**, to be published in the Proceedings of the XIth International Conference of Gas

Discharges and Their Applications, Tokyo, Japan, September 11-15, 1995.

The rates for production of the compounds  $S_2OF_{10}$ , and  $S_2OF_{10}$ , and  $S_2O_2F_{10}$  have been measured both in spark and continuous, constant-current (40  $\mu A$ ) negative glow corona discharges generated using point-to-plane electrode gaps in "pure"  $SF_6$  and  $SF_6/O_2$  gas mixtures containing different relative amounts of oxygen, up to 10%. The measurements were performed for total gas pressures in the range of 100 kPa to 200 kPa, and the  $SF_6$  discharge byproduct concentrations were measured using a gas chromatograph-mass spectrometric technique and a cryogenic enrichment chromatographic technique, respectively, for the corona and spark experiments. When  $O_2$  is added to the gas, there is a dramatic drop in the  $S_2F_{10}$  yield from both types of discharges with a corresponding increase in  $S_2OF_{10}$  yield from the spark and  $S_2O_2F_{10}$  yield from the corona discharge. The results can be explained within the framework of a plasma-chemical model from considerations of the competition among the reactions of  $SF_5$  radicals produced by dissociation of  $SF_6$  in the discharge with  $SF_5$  itself as well as with  $O_2$  and  $O$ , and the relative degree of  $O_2$  dissociation in the two types of discharges.

[Contact: Richard J. Van Brunt, (301) 975-2425]

### Power Systems Metrology

#### Recently Published

Misakian, M., and Fenimore, C., **Three-Axis Coil Probe Dimensions and Uncertainties During Measurement of Magnetic Fields from Appliances**, Journal of Research of the National Institute of Standards and Technology, Vol. 99, No. 3, pp. 247-253 (May-June 1994).

Comparisons are made between the average magnetic flux density for a three-axis circular coil probe and the flux density at the center of the probe. The results, which are determined assuming a dipole magnetic field, provide information on the uncertainty associated with measurements of magnetic fields from some electrical appliances and other electrical equipment. The present investigation extends an earlier treatment of the problem, which did not consider all orientations of

the probe. A more comprehensive examination of the problem leaves unchanged the conclusions reached previously.

[Contact: Martin Misakian, (303) 497-2426]

Morrison, H.D., Chu, F.Y., Eygenraam, M., Sauers, I., and Van Brunt, R. J., **Decomposition of  $SF_2F_{10}$  in Power ARCS**, Proceedings of the Seventh International Symposium on Gaseous Dielectrics, Knoxville, Tennessee, April 24-28, 1994 (March 1995).

Decomposition of  $SF_6$  in electrical discharges produces many toxic solids and gases.  $S_2F_{10}$  is the most toxic of the gaseous byproducts and has been found in arcs, sparks, and corona. Of these,  $S_2F_{10}$  production in arcs is the least understood, in part because  $S_2F_{10}$  is known to decay rapidly at temperatures above 250 °C. As temperatures in an arc are considerably higher, it is believed that  $S_2F_{10}$  cannot be formed directly by an arc. The first experiments where  $S_2F_{10}$  was detected in  $SF_6$  decomposed by a power arc employed a burn-through configuration into another chamber containing  $SF_6$  at a lower pressure. In those experiments, the  $S_2F_{10}$  may have been formed during the volume expansion and cooling of the  $SF_6$  decomposition products into the second chamber. We have conducted a series of tests of a power arc discharge contained completely within a bus duct configuration. Among the many other gaseous byproducts, we have detected  $S_2F_{10}$  at or below the part per million (ppm) by volume level, proving that  $S_2F_{10}$  can be formed directly by a power arc within  $SF_6$ -insulated equipment. The relative production rate of  $S_2F_{10}$  with respect to that of  $SOF_2$  and  $SF_4$ , however, implies that  $S_2F_{10}$  is not a significant contributor to the hazard of exposure to decomposed  $SF_6$ .

[Contact: Richard J. Van Brunt, (301) 975-2425]

Olthoff, J.K., and Van Brunt, R.J., **Decomposition of Sulfur Hexafluoride by X-Rays**, Proceedings of the Seventh International Symposium on Gaseous Dielectrics, Knoxville, Tennessee, April 24-28, 1994, pp. 417-422 (March 1995).

The decomposition of gaseous sulfur hexafluoride ( $SF_6$ ) by exposure to high-energy photons, and the subsequent formation of toxic and corrosive oxyfluoride by-products, is of interest due to the use

of SF<sub>6</sub> as a high-voltage insulator near sources of radiation, such as particle accelerators and X-ray units. Additionally, information about by-product formation due to radiation exposure can be compared with data obtained for the volume in which the decomposition occurs usually many orders of magnitude larger for radiation exposure than for electrical discharges. However, little previous work has been done to determine the effects of radiation upon gaseous SF<sub>6</sub>.

In this paper, we present results of by-product formation in gaseous SF<sub>6</sub> exposed to high-energy X-rays. The identity and concentration of the decomposition by-products are determined by gas chromatography/mass spectrometry techniques that were developed to investigate the decomposition of SF<sub>6</sub> exposed to corona discharges. The production curves of SOF<sub>2</sub> and S<sub>2</sub>F<sub>10</sub> are determined for a range of SF<sub>6</sub> gas pressures, X-ray energies, and X-ray fluxes. Evidence for the presence of other by-products, such as SOF<sub>4</sub>, SO<sub>2</sub>F<sub>2</sub>, and S<sub>2</sub>O<sub>2</sub>F<sub>10</sub> is also presented. The decomposition data for the SF<sub>6</sub> exposed to X-rays are compared with previously published data for the SF<sub>6</sub> exposed to corona discharges.

[Contact: James K. Olthoff, (301) 975-2431]

Slowikowska, H., Las, T., Slowikowski, J., and Van Brunt, R.J., **Modification of Cast Epoxy Resin Surfaces during Exposure to Partial Discharges**, Proceedings of the Seventh International Symposium on Gaseous Dielectrics, Knoxville, Tennessee, April 24-28, 1994, pp. 635-642.

Various techniques have been used to quantify the effects of local partial-discharge activity in changing the roughness, morphology, and resistivity of cast epoxy resin surfaces. Measurements were performed on different types of epoxy materials with and without Al<sub>2</sub>O<sub>3</sub> filler that had been exposed to partial discharge in point-dielectric gaps in either air or controlled gas mixtures for up to 24 h. In all cases, exposure to partial discharge was found to cause a significant local decrease in surface resistivity and to remove material at the discharge site, resulting in an increase of surface roughness. [Contact: Richard J. Van Brunt, (301) 975-2425]

Van Brunt, R.J., von Glahn, P.G., and Las, T., **Influence of Surface Charge on the Stochastic**

**Behavior of Partial Discharge in Dielectrics**, Proceedings of the 2nd International Conference on Space Charge in Solid Dielectrics, Antibes-Juan-Les-Pins, France, April 2-7, 1995, pp. 439-446.

It can be shown from measurement of various conditional and unconditional discharge pulse phase, amplitude, and integrated-charge distributions that the stochastic behavior of pulsating partial-discharge phenomena which occur in proximity to solid dielectric surfaces is largely controlled by memory effects associated with charge deposition and transport on the dielectric surface. A stochastic theory of partial discharge is presented that includes effects of dielectric surface charging and charge decay on the probability of discharge pulse initiation and growth. Examples of new experimental results on the stochastic properties of partial discharge are presented for discharges generated using a point electrode in contact with solid Al<sub>2</sub>O<sub>3</sub> of different purity in air. The stochastic behavior of PD shows a dramatic sensitivity to the impurity content of Al<sub>2</sub>O<sub>3</sub>.

[Contact: Richard J. Van Brunt, (301) 975-2425]

#### Magnetic Materials and Measurements

Released for Publication

Russeck, S.E., Cross, R.W., Sanders, S.C., and Oti, J.O., **Size Effects in Submicron NiFe/Ag GMR Devices**.

We have measured the magnetoresistive response of submicrometer NiFe/Ag giant magnetoresistive (GMR) devices as a function of current density and field angle. In addition to magnetostatic broadening, we observe large jumps in the magnetoresistive response (Barkhausen jumps) due to domain switching. These effects lead to irregular device-specific magnetoresistive response curves. The large Barkhausen jumps are more pronounced at low-current density, while at high-current densities, the response is smoother due to self-field stabilization. The detailed structure of the Barkhausen jumps is very sensitive to angle of the applied magnetic field. These effects are general properties of a wide class of GMR materials that rely on incoherent reversal of many small magnetic domains. The experimental data are compared with

a micromagnetic simulation which incorporates a phenomenological GMR transport model. The model qualitatively describes the experimental data and provides insight into the detailed micromagnetic behavior of these films.

[Contact: Stephen E. Russek, (303) 497-5097]

### Magnetic Materials and Measurements

#### Recently Published

Goldfarb, R.B., **Panel Discussion on Units in Magnetism**, Magnetic and Electrical Separation, Vol. 6, pp. 105-116 (1995). [Also published in the IEEE Magnetic Society Newsletter, Vol. 31, No. 4 (October 1994).]

An evening panel discussion on magnetic units, attended by 150 participants, was held at the 1994 Joint MMM-Intermag Conference in Albuquerque, New Mexico, USA. The session was organized by C.D. Graham, Jr., and moderated by R.B. Goldfarb. The panel members were asked to describe the use of magnetic units in their countries, and to make appropriate comments and recommendations. In addition to units, several panelists talked about distinction between magnetic induction  $B$  and magnetic field-strength  $H$ , and the conversion of equations. After the panelists' opening statements, the floor was opened for questions and discussion from the audience. The panelists' summaries of their remarks are included. By agreement with authors, this article is not subject to copyright.

[Contact: Ronald B. Goldfarb, (303) 497-3650]

### Superconductors

#### Released for Publication

Ceremuga, J., Krupka, J., Geyer, R.G., and Modelski, J., **Influence of Film Thickness and Air Gaps in Surface Impedance Measurements of High Temperature Superconductors Using the Dielectric Resonator Technique.**

[See Electromagnetic Properties.]

Roshko, A., Goodrich, L.F., Rudman, D.A., Moerman, R., and Vale, L.R., **Magnetic Flux Pinning in Epitaxial  $\text{YBa}_2\text{Cu}_3\text{O}_{7-\delta}$  Thin Films.**

[See Cryoelectronic Metrology.]

### Superconductors

#### Recently Published

Cooley, L.D., and Grishin, A.M., **Pinch Effect in Commensurate Vortex-Pin Lattices**, Physical Review Letters, Vol. 74, No. 14, pp. 2788-2791 (April 1995).

The critical state in a superconductor with periodic pins has properties similar to the pinch effect, known in plasma physics. It forms a terrace structure around the average flux density gradient, causing stratification of the transport current into the terrace edges where the flux density gradient is large. Regions of extremely high current, thus, interlace with regions of near zero current. The appearance of each new terrace inside the superconductor causes the magnetization to change abruptly at rational or periodic fields. This magnetization jump, a new quantum effect in superconductors, corresponds to the addition of one flux quantum threading the pin lattice unit cell.

[Contact: Lance D. Cooley, (303) 497-7747]

de Obaldia, E.I., Ludwig, K.R., Jr., Berkowitz, S.J., Clark, A.M., Skocpol, W.J., Mankiewich, P.M., Rudman, D.A., Roshko, A., Moerman, R., Vale, L., and Ono, R.H., **Coexistence of Grains with Differing Orthorhombicity in High Quality  $\text{YBa}_2\text{Cu}_3\text{O}_{7-\delta}$  Thin Films**, Applied Physics Letters, Vol. 65, No. 26, pp. 3395-3397 (December 1994).

High-quality films of  $\text{YBa}_2\text{Cu}_3\text{O}_{7-\delta}$  on  $\text{LaAlO}_3$  have been grown by pulsed-laser deposition at oxygen pressures of 3.4 to 54 Pa (25 to 400 mTorr). X-ray diffraction reveals the coexistence of grains that align with the substrate axes (axial grains) and grains that are rotated by  $0.4^\circ$  from the substrate axes (diagonal grains). The axial grains are tetragonal while the diagonal grains achieve lattice parameters close to bulk  $\text{YBa}_2\text{Cu}_3\text{O}_7$ . The relative proportion of axial grains accounts for the measured variations of normal-state conductance and superconducting critical current density from film to film, based on a simple two-dimensional model of randomly positioned, insulating axial grains.

[Contact: David A. Rudman, (303) 497-5081]

Goodrich, L.F., Wiejaczka, J.A., Srivastava, A.N., and Stauffer, T.C., **Superconductor Critical Current Measurement Standards for Fusion Applications**, NISTIR 5027 (November 1994).

This report describes research conducted to help establish a standard critical current measurement technique for Nb<sub>3</sub>Sn wires that may be used in fusion applications. The main part of this report is a detailed presentation of results of the first ITER international interlaboratory comparison of Nb<sub>3</sub>Sn critical current measurements. A common procedure and a common reaction and measurement mandrel was used by U.S. laboratories in this comparison, whereas there was no common procedure followed by other international laboratories. The largest difference in I<sub>c</sub> measurements of two laboratories that did not use a common procedure was 23%. The largest difference in I<sub>c</sub> measurements of two laboratories that did use a common procedure was 6.5%. There may still be room for improvement, but this indicates the strong need for a common detailed procedure. Results on the homogeneity of one of the Nb<sub>3</sub>Sn wires used in this study and a commentary on creating a Nb<sub>3</sub>Sn Reference Wire are also presented.

[Contact: Loren F. Goodrich, (303) 497-3143]

## ELECTROMAGNETIC INTERFERENCE

### Conducted EMI

Released for Publication

Martzloff, F.D., **Keeping Up with the Reality of Today's Surge Environment**, to be published in the Proceedings of the 1995 Power Quality/Mass Transit Conference, Ventura, California, September 11-15, 1995.

[See Power Systems Metrology.]

### Radiated EMI

Released for Publication

Camell, D.G., and Ma, M.T., **Data Evaluation of a Linear System by a Second-Order Transfer Function**, to be published in the Conference Record of the 1995 IEEE Electro-Magnetic

Compatibility Symposium, Atlanta, Georgia, August 14-18, 1995.

A recently developed technique for predicting the response of a linear system to an electromagnetic pulse, based only on the measured continuous-wave (cw) magnitude, is applied to a particular system as a case study. The measured magnitude representing the system's transfer function is deduced first from the measured response to a known cw source, supplied by the Naval Surface Warfare Center. Then, an analytic expression is derived for the magnitude square of the transfer function to approximate the measured data, and a system transfer function in terms of the complex frequency is obtained. Finally, the system's cw phase characteristics and its multiple solutions due to a given impulse source are predicted.

[Contact: Dennis G. Camell, (303) 497-3214]

Hill, D.A., Camell, D.C., Cavcey, K.H., and Koepke, G.H., **Radiated Emissions and Immunity of Microstrip Transmission Lines: Theory and Measurements**, to be published as NIST Technical Note 1377.

Radiation from a microstrip transmission line is analyzed and total radiated power calculated by numerical integration. Reverberation chamber methods for measuring radiated emissions and immunity are reviewed and applied to three microstrip configurations. Measurements from 200 to 2000 MHz are compared with theory, and excellent agreement is obtained for two configurations that minimize feed cable and finite ground plane effects. Emissions measurements are found to be more accurate than immunity measurements because the impedance mismatch of the receiving antenna cancels when the ratio of the microstrip and reference radiated power measurements is taken. The use of two different receiving antenna locations for emissions measurements illustrates good field uniformity within the chamber.

[Contact: David A. Hill, (303) 497-3472]

### Radiated EMI

Recently Published

Randa, J.P., Gilliland, D., Gjertson, W., Lauber, W.,

and McInerney, M., **Catalogue of Electromagnetic Environment Measurements, 30-300 Hz**, IEEE Transactions on Electromagnetic Compatibility, Vol. 37, No. 1, pp. 26-33 (February 1995).

The IEEE Electromagnetic Compatibility Society's Technical Committee on Electromagnetic Environments (TC-3) has undertaken a long-term project to compile an inventory or catalogue of published measurements of electromagnetic environments. The frequency spectrum has been divided into tractable bands which will be considered one at a time. We have now completed the 30- to 300-Hz band. This paper presents the resulting bibliography, along with a brief overview of what has been measured.

[Contact: James P. Randa, (303) 497-3150]

## PRODUCT DATA SYSTEMS

Released for Publication

Reid, E., and Parks, C.H., **Operating Procedures and Life Cycle Documentation for the Initial Graphics Exchange Specification**, to be published as NISTIR 5666.

This document provides a record of the underlying rationale and the detailed procedures by which the Initial Graphics Exchange Specification (IGES) is changed, new versions are approved, and the document itself is edited, maintained, and published by the IGES Project of the IGES/PDES Organization (IPO). This document also defines the life cycle documentation supporting these activities and provides guidance for its use, including record-keeping requirements, to provide evidence of compliance with these procedures.

Procedures given in this document are intended to be supplementary to and consistent with the documented procedures of the General Assembly of the IPO for the IGES Project. In general, procedures in this document are at a more detailed, working level. The methods detailed in this document have provided the IGES community with an advanced visibility of the changes approved by the organization. Through this process, each technical change reaches consensus separately,

and is held for incorporation into the subsequent version of IGES. The process still is being improved through hypertext on Internet, thereby providing the organization with timely response to proposals for extensions and repairs needed by implementors and users of IGES.

[Contact: Curtis H. Parks, (301) 975-3517]

## VIDEO TECHNOLOGY

Released for Publication

Bechis, D.J., Grote, M.D., Bortfeld, D.P., Hammer, L.H., Polak, M.J., Kelley, E.F., Jones, G.R., and Boynton, P.A., **Display Measurement Round-Robin**, to be published in the Conference Digest of the 1995 Society for Information Display International Symposium, Orlando, Florida, May 21-26, 1995.

Display measurement procedures intended for use by other laboratories and by industry for measuring, analyzing, and reporting the performance of display monitors are tested through the round-robin process in preparation for acceptance of the procedures as a standard. The NIDL and NIST results presented here show much quantitative agreement in support of the measurement procedures. Interpretation of the few discrepancies will be the subject of a later report, along with any attendant proposed refinements to the measurement and reporting procedures.

[Contact: Edward F. Kelley, (301) 975-3842]

Kelley, E.F., Jones, G.R., Boynton, P.A., Grote, M.D., and Bechis, D.J., **A Survey of the Components of Display Measurement Standards**, to be published in the Conference Digest of the 1995 Society for Information Display International Symposium, Orlando, Florida, May 21-26, 1995.

Several display standards are reviewed and distinctive elements are compared. With flat-panel displays becoming more common and the CRT displays being so well established, the associated standards activities can be somewhat bewildering, even overwhelming. This paper attempts to identify complementary and inconsistent elements of related display standards.

[Contact: Edward F. Kelley, (301) 975-3842]



## VIDEO TECHNOLOGY

### Recently Published

Fenimore, C., Field, B.F., Frank, H., Georg, E., Papillo, M., Reitmeier, G., Stackhouse, W., and Van Degrieff, C., **Report on the Workshop on Advanced Digital Video in the National Information Infrastructure**, Society of Motion Picture and Television Engineers, Inc., Vol. 104, No. 3, pp. 148-152 (March 1995). [Also published as NISTIR 5457 (July 1994)].

A workshop was held to highlight technical issues for industry and government decisionmakers with respect to Advanced Digital Video in the National Information Infrastructure (NII). The purpose of the Workshop was to: (1) define a vision of the role of digital video within the NII; (2) identify the architectural, scaling, and performance issues in realizing this vision; and (3) recommend the research, experiments, and steps to be taken to resolve these issues.

This summary by the Program Committee reports on some of the important ideas expressed by the speakers and the conclusions reached by the breakout groups, and the recommendations from the Workshop as a whole. The reader is referred to the unedited Breakout Group Reports and speakers' slides, in Part 2 of the Report, for more details. [Contact: Charles Fenimore, (301) 975-2428]

Herman, S., Field, B.F., and Boynton, P., **The Perception of Clamp Noise in Television Receivers**, Conference Record of the 1994 International Display Research Conference, Monterey, California, October 10-13, 1994, pp. 317-320.

Clamp circuits in television systems adjust the black level of each scan line to a reference voltage derived from the "back porch" of the TV signal. If the TV signal is noisy, then the derived black level can vary from scan line to scan line, resulting in a displayed streaking effect called "clamp noise." This paper reports on clamp noise research performed on a video processing supercomputer at the National Institute of Standards and Technology. This research measured the average input video signal-to-noise ratio at which human observers can

just begin to perceive clamp noise against a background of moving color pictures. This threshold was measured as a function of two parameters: two-dimensional scintillation noise due to broadband video noise, and the time constant of the clamp circuitry. These results may give TV system designers guidance in choosing tradeoffs between scintillation noise processing and clamp noise reduction.

[Contact: Bruce F. Field, (301) 975-4230]

## ADDITIONAL INFORMATION

### List of Publications

Lyons, R.M., and Gibson, K.A., **A Bibliography of the NIST Electromagnetic Fields Division Publications**, NISTIR 5028 (September 1994).

This bibliography lists publications by the staff of the National Institute of Standards and Technology's Electromagnetic Fields Division for the period from January 1970 through July 1993. Selected earlier publications from the Division's predecessor organizations are included.

[Contact: Kathryn A. Gibson, (303) 497-3132]

Meiselman, B., **Electrical and Electronic Metrology: A Bibliography of NIST Electricity Division's Publications, NIST List of Publications 94** (January 1994).

This bibliography covers publications of the Electricity Division, Electronics and Electrical Engineering, Laboratory, NIST, and of its predecessor sections for the period January 1968 to December 1993. A brief description of the Division's technical program is given in the introduction.

[Contact: Katherine H. Magruder, (301) 975-2401]

Smith, A.J., **Metrology for Electromagnetic Technology: A Bibliography of NIST Publications**, NISTIR 5029 (September 1994).

This bibliography lists the publications of the personnel of the Electromagnetic Technology Division of NIST during the period from January 1970 through publication of this report. A few earlier references that are directly related to the present work of the Division are also included.

[Contact: Annie Smith, (303) 497-3678]

Walters, E.J., **National Semiconductor Metrology Program, 1990-1994, NIST List of Publications 103** (March 1995).

This List of Publications includes all papers relevant to semiconductor technology published by NIST staff, including work of the National Semiconductor Metrology Program, the Semiconductor Electronics Division, and other parts of NIST having independent interests in semiconductor metrology. Bibliographic information is provided for publications from 1990 through 1994. Indices by topic area and by author are provided. Earlier reports of work performed by the Semiconductor Electronics Division (and its predecessor divisions) during the period from 1962 through December 1989 are provided in NIST List of Publications 72.

[Contact: E. Jane Walters, (301) 975-2050]

#### 1995 Calendar of Events

##### **October 8-12, 1995 (Orlando, Florida)**

**Special Session on Model Validation, 1995 IEEE-IAS Annual Meeting.** The Power Electronics Devices and Components Committee of the IEEE Industry Applications Society in cooperation with the NIST Working Group on Model Validation will hold a special session on model validation. This session is being introduced to reflect the growing needs and interest in establishing procedures for the comprehensive evaluation of circuit simulator models. Topics of interest include: characterization procedures that could be applied for evaluation of models, methods for identifying and implementing model validation procedures, and the application of validation procedures in comparing specific models. [Contact: Allen R. Hefner, (301) 975-2071]

##### **October 26, 1995 (Austin, Texas)**

**National Ion Implant Users Meeting.** The Ion Implant Users Group (East Coast) and the Greater Silicon Valley Implant Users Group have joined together for the first meeting on a national level. This year's meeting on the needs, challenges, approaches, modeling, and results for low-energy implantation will be held in Austin, Texas, on October 26, 1995, in conjunction with SEMI's

SEMICON/Southwest 95.

The meeting provides a forum for the informal exchange of information and ideas on ion-implant-related issues, future trends, and applications. Low-energy topics to be discussed range from practical semiconductor manufacturing issues to developmental doping techniques. These tie in directly with the SIA Roadmap for the fabrication of submicrometer structures envisioned in the next generation of computer CPUs and DRAMs. Presentations on other applications of low-energy implantation such as the treatment of space-age and medical materials for improved strength and corrosion resistance are also planned.

[Contact: John Albers, (301) 975-2075]

#### EEEL Sponsors

National Institute of Standards and Technology  
Executive Office of the President

U.S. Air Force

Hanscom Air Force Base; Newark Air Force Base; McCellan Air Force Base; Patrick Air Force Base; CCG-Strategic Defense Command; CCG-Systems Command; Wright Patterson

U.S. Army

Fort Belvoir; Redstone Arsenal; Combined Army/Navy/Air Force (CCG)

Department of Defense

Advanced Research Projects Agency; Defense Nuclear Agency; National Security Agency

Department of Energy

Building Energy R&D; Energy Systems Research; Fusion Energy; Basic Energy Sciences

Department of Justice

Law Enforcement Assistance Administration;

U.S. Navy

CCG/Seal Beach; Office of Naval Research; Naval Surface Warfare Center; Naval Air Systems Command

National Aeronautics and Space Administration

NASA Headquarters

Department of Transportation

National Highway Traffic Safety Administration

MMIC Consortium

Nuclear Regulatory Commission

Department of Health and Human Services

National Institutes of Health

Various Federal Government Agencies

## NIST SILICON RESISTIVITY SRMs

In response to needs of the semiconductor industry, NIST's Semiconductor Electronics Division provides silicon bulk resistivity Standard Reference Materials (SRMs) through the NIST Standard Reference Materials Program. A new class of resistivity SRMs is being introduced to respond better to users' requirements.

The first NIST (then NBS) resistivity SRMs were fabricated from crystal 50 mm (2 in) in diameter. These wafers represented various combinations of crystal growth process, crystallographic orientation, and doping, each combination chosen to give the best expected wafer uniformity for a given resistivity level. Each wafer in every set was individually measured and certified. Some of these sets are still available until the supply is exhausted (see table).

The Division is now certifying single-wafer resistivity standards at approximately the same resistivity values as were available in the earlier sets. These new SRMs are fabricated from crystal 100 mm in diameter, intended to provide improved compatibility with newer end-use instrumentation. In response to user comments, the new SRMs will be more uniform in both thickness and resistivity, will have reduced uncertainty of certified value due to use of an improved certification procedure using a four-point probe, and will be measured and certified at additional measurement sites for better characterization of wafer uniformity at its core. The additional measurements needed to qualify the improved SRMs will make them more expensive on a per-wafer basis than the earlier sets.

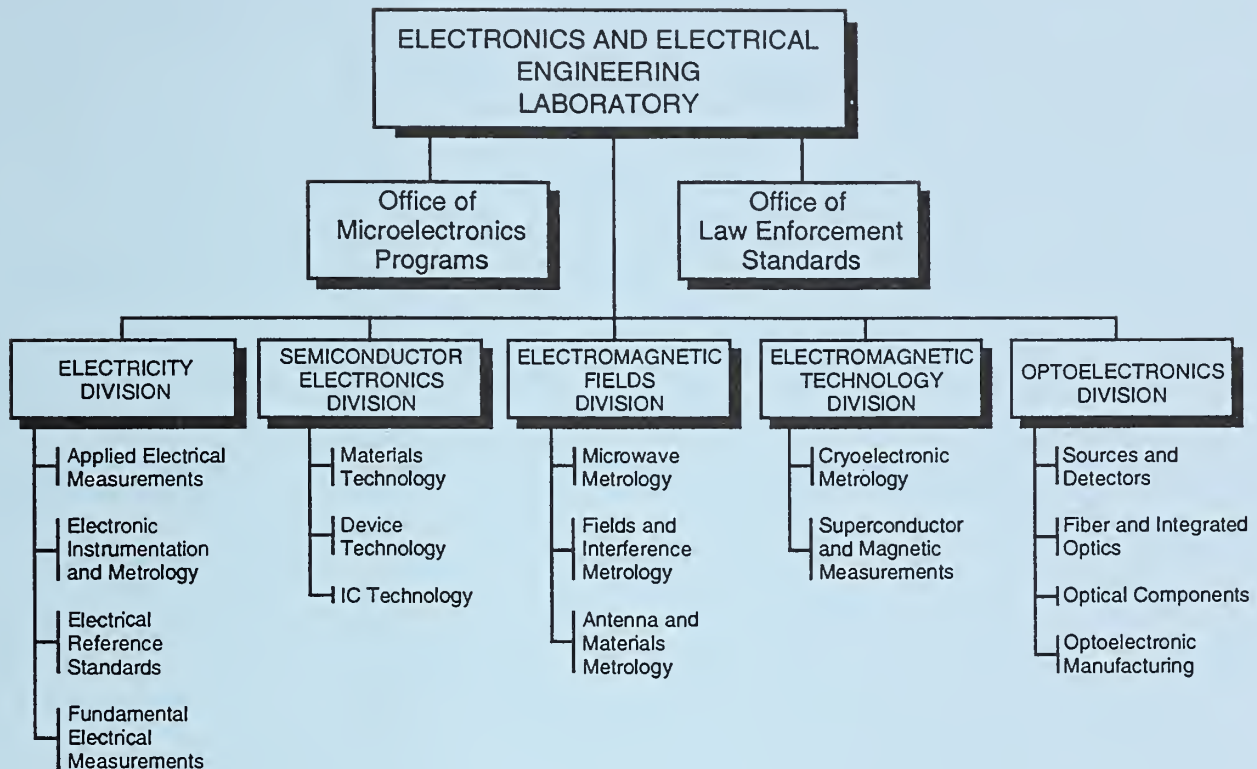
| <b><i>NIST SILICON BULK RESISTIVITY STANDARD REFERENCE MATERIALS</i></b>  |                                 |   |                        |                                 |
|---|---------------------------------|---|------------------------|---------------------------------|
| <b>DATE UPDATED: 10 MARCH 1995</b>  |                                 |   |                        |                                 |
| <b><i>Note: Problems in producing and certifying new SRMs have resulted in substantial delays. The first to become available, for 10 and 180 ohm · cm, are not likely to be ready until 1995.</i></b> |                                 |   |                        |                                 |
| <b>NOMINAL RESISTIVITY<br/>(ohm · cm)</b>   | <b><u>OLD SRMs</u></b>          | <b>AVAILABILITY</b>                         | <b><u>NEW SRMs</u></b> | <b>ANTICIPATED AVAILABILITY</b> |
| 0.01  | 1523 (one of set of two wafers) | limited supply                              | 2541                   | to be announced                 |
| 0.1   | 1521 (one of set of two wafers) | limited supply                              | 2542                   | to be announced                 |
| 1   | 1523 (one of set of two wafers) | limited supply                              | 2543                   | to be announced                 |
| 10  | 1521 (one of set of two wafers) | limited supply                              | 2544                   | to be announced                 |
| 25  | 1522                            | set of three wafers are no longer available | 2545                   | to be announced                 |
| 75  | 1522                            |   | 2546 (100)             | to be announced                 |
| 180   | 1522                            |   | 2547 (200)             | to be announced                 |

The above table will be updated in future issues to reflect changes in availability. Every effort will be made to provide accurate statements of availability; NIST sells SRMs on an as-available basis. For technical information, contact James R. Ehrstein, (301) 975-2060; for ordering information, call the Standard Reference Materials Program Domestic Sales Office: (301) 975-6776.









### KEY CONTACTS

|   |  |
|---|--|
| Laboratory Headquarters (810)             | Director, Judson C. French (301) 975-2220          |
|   | Deputy Director, Robert E. Hebner (301) 975-2220   |
|   | Associate Director, Alan H. Cookson (301) 975-2220 |
| Office of Microelectronics Programs       | Director, Robert I. Scace (301) 975-4400           |
| Office of Law Enforcement Standards       | Director, Kathleen M. Higgins (301) 975-2757       |
| Electricity Division (811)                | Acting Chief, William E. Anderson (301) 975-2400   |
| Semiconductor Electronics Division (812)  | Chief, Frank F. Oettinger (301) 975-2054           |
| Electromagnetic Fields Division (813)     | Chief, Allen C. Newell (303) 497-3131              |
| Electromagnetic Technology Division (814) | Acting Chief, Richard E. Harris (303) 497-3776     |
| Optoelectronics Division (815)            | Chief, Gordon W. Day (303) 497-5204                |

### INFORMATION:

For additional information on the Electronics and Electrical Engineering Laboratory, write or call:

Electronics and Electrical Engineering Laboratory  
 National Institute of Standards and Technology  
 Metrology Building, Room B-358  
 Gaithersburg, MD 20899  
 Telephone: (301) 975-2220

